HHS Public Access

Author manuscript

J Chem Theory Comput. Author manuscript; available in PMC 2018 April 27.

Published in final edited form as:

J Chem Theory Comput. 2018 January 09; 14(1): 303–318. doi:10.1021/acs.jctc.7b00899.

Binding Thermodynamics and Kinetics Calculations Using Chemical Host and Guest: A Comprehensive Picture of Molecular Recognition

Zhiye Tang and **Chia-en A. Chang***

Department of Chemistry, University of California, Riverside, California 92521, United States

Abstract

Understanding the fine balance between changes of entropy and enthalpy and the competition between a guest and water molecules in molecular binding is crucial in fundamental studies and practical applications. Experiments provide measurements. However, illustrating the binding/unbinding processes gives a complete picture of molecular recognition not directly available from experiments, and computational methods bridge the gaps. Here, we investigated guest association/dissociation with β-cyclodextrin (β-CD) by using microsecond-time-scale molecular dynamics (MD) simulations, postanalysis and numerical calculations. We computed association and dissociation rate constants, enthalpy, and solvent and solute entropy of binding. All the computed values of k_{on}, k_{off}, ΔH, ΔS, and ΔG using GAFF-CD and q4MD-CD force fields for β-CD could be compared with experimental data directly and agreed reasonably with experiment findings. In addition, our study further interprets experiments. Both force fields resulted in similar computed ΔG from independently computed kinetics rates, $\Delta G = -RT\ln(k_{on}\cdot C^0/k_{off})$, and thermodynamics properties, $\Delta G = \Delta H - T\Delta S$. The water entropy calculations show that the entropy gain of

*Corresponding Author: Phone: (951) 827-7263. chiaenc@ucr.edu.

ORCID

Zhiye Tang: 0000-0002-5092-1575

Notes

The authors declare no competing financial interest.

Supporting Information

The Supporting Information is available free of charge on the ACS Publications website at DOI: 10.1021/acs.jctc.7b00899.

Movie of association and dissociation pathways from GAFF-CD force field: β-CD-aspirin direct association (AVI)

Movie of association and dissociation pathways from GAFF-CD force field: β-CD-aspirin direct dissociation (AVI)

Movie of association and dissociation pathways from GAFF-CD force field: β-CD-aspirin sticky association (AVI)

Movie of association and dissociation pathways from GAFF-CD force field: β-CD-aspirin sticky dissociation (AVI)

Movie of association and dissociation pathways from GAFF-CD force field: β-CD-*tert*-butanol direct association (AVI)

Movie of association and dissociation pathways from GAFF-CD force field: β-CD-*tert*-butanol direct dissociation (AVI)

Movie of association and dissociation pathways from q4MD-CD force field: β-CD-aspirin direct association (AVI)

Movie of association and dissociation pathways from q4MD-CD force field: β-CD-aspirin direct dissociation (AVI)

Movie of association and dissociation pathways from q4MD-CD force field: β-CD-aspirin sticky association (AVI)

Movie of association and dissociation pathways from q4MD-CD force field: β-CD-aspirin sticky dissociation (AVI)

Movie of association and dissociation pathways from q4MD-CD force field: β-CD-*tert*-butanol direct association (AVI)

Movie of association and dissociation pathways from q4MD-CD force field: β-CD-*tert*-butanol direct dissociation (AVI)

Length of MD simulations; conformations of β-CD in vacuum MD simulations in GAFF-CD and q4MD-CD; details of enthalpy decomposition calculations; surface area, hydrogen bond, and solvation water; definition of probability distribution of conformations of solutes; solvation entropy calculation using water molar entropy; solvation water; solute concentrations used in association rate constant calculations; diffusion-controlled association rate constants estimated from diffusion coefficient; uncertainty evaluation of computed properties; experimental data of ΔG, ΔH, and $-T\Delta S$ of β-CD-alcohol complexes using ITC and UV; convergence of enthalpy calculations ($\langle E \rangle$); ligand external degrees of freedom; bound and free period lengths of the complexes; comparison of ΔG_{Comp1} and ΔG_{Comp2} (PDF)

desolvating water molecules are a major driving force, and both force fields have the same strength of nonpolar attractions between solutes and β-CD as well. Water molecules play a crucial role in guest binding to β-CD. However, collective water/β-CD motions could contribute to different computed k_{on} and ΔH values by different force fields, mainly because the parameters of β-CD provide different motions of β-CD, hydrogen-bond networks of water molecules in the cavity of free β-CD, and strength of desolvation penalty. As a result, q4MD-CD suggests that guest binding is mostly driven by enthalpy, while GAFF-CD shows that gaining entropy is the major driving force of binding. The study deepens our understanding of ligand–receptor recognition and suggests strategies for force field parametrization for accurately modeling molecular systems.

Graphical Abstract

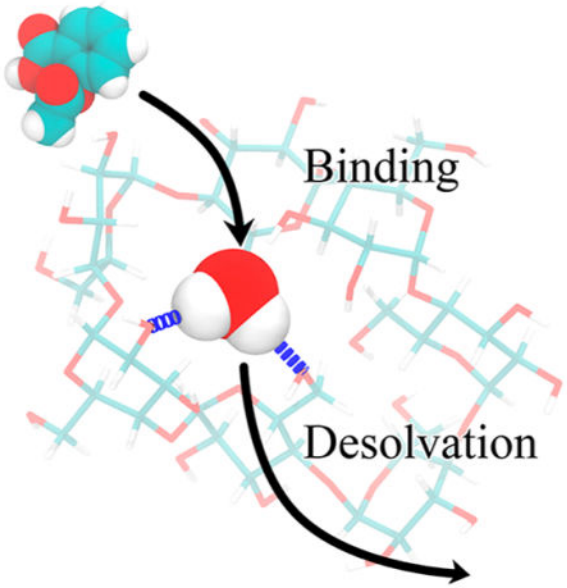

1. INTRODUCTION

Molecular recognition determines the binding of two molecules—a common phenomenon in chemical and biological processes. Thus, understanding molecular recognition is of interest in both fundamental studies and has practical applications in chemical industries and drug discovery. Molecular binding can be characterized by thermodynamic and kinetic properties, which are governed by factors such as polar and nonpolar interactions between solutes, solvent effects, molecular diffusion, and conformational fluctuations. Molecular binding affinity is a straightforward characterizer of recognition and can be obtained experimentally by enthalpimetry such as calorimetry.[1,2] However, it is difficult to measure the binding entropy directly from experiments, and it is impossible to measure separate entropy contributions from the solvent and solute. Recent studies have revealed the importance of kinetic properties[3–5] and showed that drug efficacy is sometimes correlated with the kinetic properties better than binding affinity.[6,7] Investigating residence time[8–10] was proposed in the past decade and has become a useful criterion in predicting drug efficacy. Efforts have been devoted to studies of kinetic–structure relations.[11–14] Computational methods, which

have the advantage of an atomistic resolution, are useful tools to investigate the fundamentals of thermodynamics and kinetics. With the recent breakthrough in computational powers, molecular dynamics (MD) is able to simulate up to microsecond or millisecond time scale molecular motions.[15,16] Therefore, computational methods can be used to sample a larger time scale of dynamics of host–guest systems and take advantage of numerical methods to directly extract the enthalpic and entropic profiles of both the solvent and the solute as well as the kinetics from unbiased long-time-scale MD. New findings observed from chemical host–guest systems with theoretically sound computational methods have advanced our knowledge of molecular recognition and brought new insights into ligand–protein systems.

Cyclodextrins (CDs) are a class of cyclic oligosaccharide compounds that can be obtained by degradation of starch by α-1,4-glucan-glycosyltransferases. Depending on the number of glucopyranose units (D-glucose), these compounds can be classified into 6 units (α-CD), 7 units (β-CD), 8 units (γ-CD), and CDs of more glucopyranose units. In β-CD (Figure 1), the 7 glucopyranose units (D-glucose) enclose a cavity with a diameter of about 6.5 Å. The glucopyranose units bring the center of the cavity a hydrophobic surface of the carbon chains in the glucopyranose, whereas the rims of β-CD consist of hydrophilic hydroxyl groups. Notably, the wide and narrow rims of β-CD are asymmetrical. Because of the structure and size of the cavity, β-CD can host a wide variety of guest molecules via nonpolar or polar attractions. With these properties, β-CD and its derivatives have many applications in many fields, such as the cosmetics industry, pharmaceuticals, catalysis, and food and agricultural industries.[17–23] Thus, the experimental thermodynamics and kinetics data are available for a variety of β-CD complexes.[24–30]

β-CD consists of 147 atoms, so we can directly investigate the fundamentals of binding thermodynamics and kinetics by MD simulations. Short MD simulations have been used to study ligand binding affinity, dynamics, H bonds, and hydration properties of β-CD complexes.[31–38] Replica exchange molecular dynamics (REMD) and the Mining Minima 2 method were used to thoroughly sample the bound states of various β-CD complexes and accurately evaluate their binding affinities by using an implicit solvent model.[39,40] QM/MM methods were also used to investigate the binding pose, binding enthalpy, and properties of the β-CD cavity.[41–44] In most of these studies, the conformations of β-CD resemble the crystal structures via shorter than 20 ns MD simulations and no further dynamic information from experiments or long-time-scale MD of β-CD complexes. In addition, although the binding affinity decomposition into enthalpy and entropy has been achieved for some ligands, the use of an implicit solvent model and previous computation techniques cannot obtain both solvent and solute entropy contributions that allow direct comparison with experimentally measured ΔH and ΔS. It is still difficult to sample multiple association/dissociation events for kinetic rate calculations. [45]

The present study applied microsecond-time-scale MD simulations with GPU acceleration to compute binding kinetics and thermodynamics of 7 guests with β-CD to reveal the binding mechanisms. Using two force fields for β-CD, GAFF-CD, and q4MD-CD, we performed simulations that sampled multiple association/dissociation events of the complexes to compute k_{on} and k_{off} together with MD of free β-CD and guests and a water

box to compute entropy and enthalpy from both contributions of solvent and solutes. The nonpolar interactions between solutes and the water entropy gains on binding were the major driving forces of association, regardless of the use of force fields. However, GAFF-CD provided slightly more flexible β-CD, which produced more complicated H-bond networks between the free β-CD and water molecules in the first hydration shell, thereby resulting in slower k_{on} and larger desolvation penalty. The study also gives details regarding multiple guest association and dissociation pathways and explains how each decomposed energetic and entropic term contributes to binding kinetics/thermodynamics and binding mechanisms.

2. METHOD

Molecular Systems and Force Fields

We selected 4 weak binders (1-butanol, *tert*-butanol, 1-propanol, methyl butyrate) and 3 relatively stronger binders (aspirin, 1-naphthyl ethanol, 2-naphthyl ethanol) as the guest molecules (ligands) for the β-CD host–guest complexes. Note that the 3 relatively stronger binders still bind weakly with β-CD (mM binders). The set of data has similar experimental binding affinities (ΔG) by both kinetics and thermodynamic measurements, and the available rate constants are accessible by MD for sampling multiple association and dissociation events. Structures of guests were manually created using Vega ZZ,[46] and the structure of β-CD was obtained from the Cambridge Crystal Data Center (PDB ID: WEWTOJ) (Figure 1). We used two different force fields for β-CD: Amber general force field (GAFF),[47] termed GAFF-CD, and q4MD-CD force field.[48] For simulations with GAFF-CD, we took the partial charge of β-CD from a previous work.[40] For simulations using q4MD-CD, the partial charge of β-CD was provided in the force field. The guests were modeled by only GAFF, and the partial charges were computed using optimization and then ChelpG atomic charge calculation with the Gaussian package[49] at the 6-31+g(d,p)/B3LYP level. Initial conformations of the complexes were obtained by manually locating the ligand in the center of the cavity of β-CD. All MD simulations and calculations were repeated in the same setting for the free and bound β-CD with GAFF-CD and q4MD-CD.

Molecular Dynamics Simulations

We performed microsecond- time-scale MD runs for a total of 1–11 μs simulations (Table SI 1) for each β-CD-ligand system, that is, on the complex, the free β-CD, the free ligand, and an empty water box.[50] For each run, the system was first solvated with exactly 1737 TIP3P water molecules (about 12 Å away from the solute) and then optimized to eliminate possible clashes. The water molecules were then equilibrated at 298 K for 1 ns, followed by an equilibration of the entire system from 200 to 298 K for 150 ps. By using Amber 14 with GPU acceleration, [47,51] long production runs were performed at 298 K maintained by a Langevin thermostat[52,53] in an NPT (isothermal–isobaric) ensemble. A frame was saved every 1 ps for each run. For postanalysis and numerical calculations we resaved a frame every 10 ps, and the trajectories were visualized by VMD.[54] Table SI 1 summarizes the total lengths of all MD simulations and numbers of frames used in thermodynamics calculations. We also performed 50 ns MD runs for free β-CD in a vacuum by using GAFF-CD and q4MD-CD to examine the force field parameters, as detailed in SI section 2.

Binding Enthalpy Calculation

The binding enthalpy (ΔH) was calculated by $\Delta H = \langle E \rangle_{\text{Complex}} + \langle E \rangle_{\text{Water}} - \langle E \rangle_{\text{Host}} - \langle E \rangle_{\text{Guest}}$ [50] with the periodicity of the water box, where $\langle E \rangle_{\text{Complex}}$, $\langle E \rangle_{\text{Water}}$, $\langle E \rangle_{\text{Host}}$, and $\langle E \rangle_{\text{Guest}}$ are the averaged potential energies of all molecules from the trajectories of the complex, water, host, and guest, respectively. Note that only the bound state conformations from the trajectories of the complexes were used to compute $\langle E \rangle_{\text{Complex}}$. The kinetic energy will be canceled, so it is not evaluated here. The pressure–volume term is negligible in a solvated system. The computed decomposed enthalpy terms are reported in SI section 3. We also computed the surface area, number of H bonds, and number of solvation water (detailed in SI section 4) to explain our decomposed enthalpy terms.

Solute Entropy Calculation

Solute entropy change (ΔS_{Solute}) and water entropy change (ΔS_{Water}) are computed separately for binding entropy, $\Delta S = \Delta S_{\text{Solute}} + \Delta S_{\text{Water}}$, where ΔS_{Solute} was decomposed into host internal (conformational/vibrational) entropy change (ΔS_{Host}), guest internal entropy change ($\Delta S_{\text{Guest Int}}$), and guest external (translational/rotational) entropy change ($\Delta S_{\text{Guest Ext}}$), illustrated as $\Delta S_{\text{Solute}} = \Delta S_{\text{Host}} + \Delta S_{\text{Guest Int}} + \Delta S_{\text{Guest Ext}}$.

Notably, the host retains its external degrees of freedom, so there is no change of external entropy for the host. The internal entropy changes of the host ($\Delta S_{\text{Host}} = S_{\text{Host Complex}} - S_{\text{Host Free}}$) and guest ($\Delta S_{\text{Guest Int}} = S_{\text{Guest Int Complex}} - S_{\text{Guest Int Free}}$) were calculated by taking the difference in internal entropies of their free state and bound state by using the Gibbs entropy formula (eq 1)[55,56]

$$S_{\text{Int}} = -R \int P(\Omega_{\text{Solute}}) \ln(P(\Omega_{\text{Solute}})) \mathrm{d}\Omega_{\text{Solute}} \quad (1)$$

where R is the gas constant and $P(\Omega_{\text{Solute}})$ is the probability distribution of conformations (Ω_{Solute}) defined by key dihedrals in the species, as detailed in SI section 5.

In the free states, both β-CD and ligands can diffuse freely in solution, but ligand diffusion may be restricted after binding into the cavity of β-CD. The external entropy loss of the ligand was calculated as $\Delta S_{\text{Guest Ext}} = S_{\text{Guest Ext Complex}} - S_{\text{Guest Ext Free}}$, where $S_{\text{Guest Ext Free}} = R \ln(8\pi^2/C^0)$ is approximately 6.98 kcal/mol at 298 K.[57,58] R is the gas constant, and C^0 is the standard concentration (1 M). $S_{\text{Guest Ext Complex}}$ is the external entropy of the ligands evaluated by numerical integration after aligning the MD trajectories of the complexes to the crystal structure of β-CD

$$S_{\text{GuestExtComplex}} = R \ln\left(\int \sin(\theta) \mathrm{d}x \, \mathrm{d}y \, \mathrm{d}z \, \mathrm{d}\phi \, \mathrm{d}\varphi \, \mathrm{d}\theta \right) \quad (2)$$

where x, y, and z are the Cartesian coordinates of the ligand translation and ϕ, φ, and θ are the Euler angles of the ligand rotation. The bin size of x, y, and z was 2 Å, and the bin size

of ϕ, φ, and θ was 30°. The ϕ and φ were integrated from $-\pi$ to π, and θ was integrated from $-\pi/2$ to $\pi/2$.

Water Entropy Calculation

We evaluated the water entropy change on ligand binding (ΔS_{Water}) from the solvation entropy ($\Delta S_{\text{Solv}\cdot}$) of the free β-CD ($\Delta S_{\text{Solv}\cdot\text{Host}}$), free guests ($\Delta S_{\text{Solv}\cdot\text{Guest}}$), and the complexes ($\Delta S_{\text{Solv}\cdot\text{Complex}}$) by $\Delta S_{\text{Solv}\cdot} = \Delta S_{\text{Solv}\cdot\text{Trans}} + \Delta S_{\text{Solv}\cdot\text{Rot}} + \Delta S_{\text{Solv}\cdot\text{Conf}}$. $\Delta S_{\text{Solv}\cdot}$ was calculated by the grid cell method.[59–61] In the grid cell method, the water molecules in the water box are treated as if they are vibrating in a local cell and confined by the forces from surrounding water molecules and solutes. In the cell method, $\Delta S_{\text{Solv}\cdot}$ decomposes into vibrational ($\Delta S_{\text{Solv}\cdot\text{ Vib}}$) and conformational ($\Delta S_{\text{Solv}\cdot\text{Conf}}$) entropies and $\Delta S_{\text{Solv}\cdot\text{Vib}}$ further decomposes into translational ($\Delta S_{\text{Solv}\cdot\text{Trans}}$) and rotational ($\Delta S_{\text{Solv}\cdot\text{Rot}}$) entropies. The entropy terms were calculated by using eqs 6.8–6.11 in the SI, and an in-house script was developed to perform the calculations. The changes in water entropy on ligand binding were evaluated by $\Delta S_{\text{Water}} = \Delta S_{\text{Solv}\cdot\text{Complex}} - \Delta S_{\text{Solv}\cdot\text{Host}} - \Delta S_{\text{Solv}\cdot\text{Guest}}$. The translational ($\Delta S_{\text{Water Trans}}$), rotational ($\Delta S_{\text{Water Rot}}$), and conformational ($\Delta S_{\text{Water Conf}}$) terms of changes of water entropy on ligand binding were evaluated by the same equation. The setting of solvation water entropy calculation is provided in SI section 6. We counted the number of solvation water molecules in the free guest, free host, and complexes to explain the water entropy calculations, as detailed in SI section 7.

Calculations of the Association and Dissociation Rate Constants

As mentioned previously, our MD simulations can sample multiple association and dissociation events in one long run for each system. We define the bound state for a complex when the center of mass of the ligand is within 7.5 Å from the center of mass of β-CD. Any bound/unbound period that lasted longer than 1.0 ns was counted as one bound/unbound event. Because molecules fluctuate during ligand binding, if a ligand stayed or left β-CD for less than 1.0 ns, we did not consider the motion as a bound/unbound event. The average bound/unbound period lengths were calculated and plugged into eqs 3 and 4 to compute k_{on} and k_{off}, where [solute] is the concentration of solute estimated by the averaged size of the water box, as detailed in SI section 8. After obtaining k_{on} and k_{off}, we calculated the equilibrium constant $K_{\text{eq}} = k_{\text{on}}/k_{\text{off}}$. We also estimated the diffusion-controlled association rate constants by using diffusion coefficients and radii of host and guest molecules for comparison, as detailed in SI section 9.

$$k_{\text{on}} = \frac{1}{\text{average unbound time} \times [\text{solute}]} \quad (3)$$

$$k_{\text{off}} = \frac{1}{\text{average bound time}} \quad (4)$$

Binding Free Energy Calculation

The binding free energies can be computed by using the classical thermodynamics and statistical mechanics equations. We evaluated binding free energies (ΔG_{Comp1}) from the computed binding enthalpy and binding entropy as in eq 5. We also evaluated binding free energies (ΔG_{Comp2}) from the computed association and dissociation rate constants (k_{on} and k_{off}) as in eq 6

$$\Delta G_{\text{Comp1}} = \Delta H - T\Delta S \quad (5)$$

$$\Delta G_{\text{Comp2}} = -RT \ln (k_{\text{on}} \cdot C^0/k_{\text{off}}) \quad (6)$$

Uncertainty Evaluation of Computed Properties

We evaluated the uncertainties of the binding enthalpy (ΔH), the entropy change of water (ΔS_{Water}), the internal entropy change of β-cyclodextrin (ΔS_{Host}), the internal ($\Delta S_{\text{Guest Int}}$) and external ($\Delta S_{\text{Guest Ext}}$) entropy change of guests, the total binding entropy (ΔS), the binding free energy from eq 5 (ΔG_{Comp1}), the association (k_{on}) and dissociation (k_{off}) rate constants, and the equilibrium constant (K_{eq}). The details are provided in SI section 10.

3. RESULTS

We used microsecond-time-scale MD simulations with an explicit solvent model to compute the binding enthalpies, entropies, and association/dissociation rate constants for β-CD with 7 guest molecules (Figure 1). Binding free energy ΔG was computed by using eq 5 (ΔG_{Comp1}), from the thermodynamic properties, and eq 6 (ΔG_{Comp2}), from the kinetics binding rate constants. All computed results yielded reasonable agreement with experimental data (Tables 1 and 2 and Figure 2). Two force fields, GAFF-CD and q4MD-CD, were used to assign parameters for β-CD, and all ligands used the GAFF force field. In general, ΔG computed with GAFF-CD is slightly more positive than the experimental data, and binding is driven by entropy. In contrast, q4MD-CD yields slightly more negative computed ΔG than experimental data, and binding is driven by enthalpy. Here we were able to separate enthalpy and entropy calculations, and we therefore use directly computed ΔH and $-T\Delta S$ to investigate their contributions of a guest and β-CD binding.

Binding Enthalpy and Entropy Calculations

The calculated ΔH, $-T\Delta S$, and ΔG_{Comp1} by using eq 5 with the GAFF-CD and q4MD-CD force fields are compared with the experimental data in Table 1. The computed ΔG is mostly within 2 kcal/mol of experiments, and they provide a correct trend. Although results from the two force fields reasonably agree with experimental results, GAFF-CD generally underestimated and q4MD-CD overestimated the binding free energy. The intermolecular van der Waals (vdW) attraction between β-CD and a guest is one major driving force for complex formation (Tables 3 and 4) as well as the water entropy gain on binding (Table 5).

Interestingly, compared to q4MD-CD, the less negative binding affinities using GAFF-CD are primarily from the larger desolvation penalty, resulting in the less negative binding enthalpy. The host became more flexible and gained configuration entropy on binding, which is another favorable factor in guest binding (Table 5). In contrast, as compared with GAFF-CD, q4MD-CD modeled a significantly smaller desolvation penalty and more negative ΔH, which become the main driving force for binding. However, the systems need to pay a higher cost in entropy ($-T\Delta S$) because the host became more rigid in the bound state.

Unlike for experiments and most calculations that measured ΔG and ΔH, we independently computed ΔH and $-T\Delta S$. Nevertheless, we still observed entropy–enthalpy compensation in our systems with different force fields, so the compensation in these systems indeed has a physical implication and is not an artifact from the mathematics of eq 5. We compared the calculated ΔH and $-T\Delta S$ for 1-propanol and 1-butanol for which experimental data are available. Both experiments and calculations with GAFF-CD showed a small positive ΔH, which slightly opposed binding, but the systems gained more entropy to compensate for losing enthalpy on binding. Although only 2 guests studied here have experimental ΔH and $-T\Delta S$, the binding data for other alcohols of β-CD with calorimetry (ITC) and UV experiments commonly show gaining entropy, and enthalpy was not the predominant determinant for binding in all cases (Figure SI 7). The following subsections present results of the binding enthalpy of solute–solute and solute–solvent and the binding entropy of solutes and solvent.

Changes of Enthalpy from Different Components

We evaluated the absolute values of binding enthalpy by using potential energies $\langle E \rangle$ from microsecond-time-scale MD trajectories of the four species, and the convergences of the enthalpy calculations were first examined (Figures SI 8–10). For all simulations, the potential energy reaches a stable value within a fluctuation of 0.4 kcal/mol, which is also within reported experimental uncertainty.[24,28,29,62,63] The fluctuations of potential energies of β-CD-1-propanol, β-CD-1-butanol, and β-CD-*tert*-butanol complexes are larger with GAFF-CD than the other systems. The fractions of the bound states of these systems are lower than with the other systems; thus, the smaller numbers of sampling result in larger fluctuations.

To understand binding enthalpies, we decomposed the calculated values into various contributions (Table 3). We also provide the decompositions into vdW and Coulombic interactions for $\Delta H_{\text{Solute Inter}}$, $\Delta H_{\text{Host Conf}}$, $\Delta H_{\text{Host–Water}}$, and $\Delta H_{\text{Guest–Water}}$ (Tables 4, 6, and 7). Regardless of the type of force field used, we immediately noticed that $\Delta H_{\text{Host–Guest}}$ data are all favorable (negative), and stronger binders such as naphthyl ethanol and aspirin have large negative $\Delta H_{\text{Host–Guest}}$ value,~–30 kcal/mol (Table 3). However, $\Delta H_{\text{Desolvation}}$ largely compensates for the solute–solute attraction, for significantly smaller ΔH, ranging from 3.0 to −1.4 kcal/mol with GAFF-CD and from −0.9 to −5.7 kcal/mol with q4MD-CD. The computed ΔH with GAFF-CD yielded positive values for weak binders ($\Delta G > -2.0$ kcal/mol), which has been seen in experiments (see Figure SI 7). In contrast, ΔH values are all negative with q4MD-CD. On binding, both β-CD and the guest desolvate water molecules

and lose interactions with water molecules; thus, $\Delta H_{\text{Host–Water}}$ and $\Delta H_{\text{Guest–Water}}$ values are all positive. The values are larger for stronger binders; presumably, guests such as naphthyl ethanols have larger sizes as compared with weaker/small binders such as propanol. The water molecules released after binding regain interactions with other water molecules, thereby resulting in all negative $\Delta H_{\text{Water–Water}}$ values. However, this term is not negative enough to counterbalance the loss from water–solute interactions. As a result, desolvation enthalpy is inevitably all positive and becomes the major force that opposes binding. Of note, the desolvation penalty from the polar contribution is the major force that opposes binding with GAFF-CD, which results from losing more intermolecular H bonds between water molecules and β-CD (Table 7). The partial charges and the nonpolar attractions between guests and β-CD modeled with both force fields are highly similar. However, different parameters for the bonded terms result in different modeled β-CD conformations, which significantly changes the H-bond networks between water molecules and β-CD. As illustrated in Figure 3 and Table SI 2, the conformation results in breaking more intermolecular H bonding and larger desolvation penalty in GAFF-CD on guest binding.

Strong enough intermolecular attraction $\Delta H_{\text{Solute Inter}}$ is always required for molecular recognition, and vdW attraction was the major driving force for all guests (Table 4). The loss of intramolecular H bonds of β-CD on guest binding is compensated by the intermolecular Columbic attraction in the bound state ($\Delta H_{\text{Host Conf (Coul)}}$ in Table 6). Although the values of $\Delta H_{\text{Host–Guest}}$ with both force fields are similar, the decomposition shows significantly larger numbers of each contribution to $\Delta H_{\text{Host Conf}}$, such as $\Delta H_{\text{Host Conf (vdW)}}$ and $\Delta H_{\text{Host Conf (Coul)}}$ of β-CD, with GAFF-CD (Table 6) because of larger conformational changes after ligand binding. The free β-CD prefers flipping 2 glucopyranose units instead of holding an open cavity, as shown in the crystal structure (Figure 4, GAFF-CD free β-CD a and c compared to low population of b). The glucose rings flipped outward during ligand binding, which lost more water molecules to allow the binding site of β-CD to be accessible for guests to bind. In contrast, q4MD-CD appeared to have crystal-like host structures in both the free and the bound states. Note that in vacuum, both GAFF-CD and q4MD-CD sampled predominantly crystal-like host structures (Figure SI 1), which indicates that the glucose ring flipping is largely induced by the hydration shell. GAFF-CD not only changed host conformations upon ligand binding but also makes the host more flexible.

Changes of Solute Entropy on Ligand Binding

Solute entropy, also termed configuration entropy, reflects the flexibility of a molecular system. Here we used numerical integration to compute each entropy term by eq 1 for internal (conformational/vibrational) and eq 2 for external (translational/rotational) solute entropy. We used the well-defined dihedral distribution analyzed from our MD trajectories to compute internal solute entropy, as detailed in SI section 5. For the small and weak binding guests studied here, the internal solute entropy of a guest is nearly identical when the guest is in the free solution or bound to β-CD, suggesting a weak correlation between internal degrees of freedom and external translational and rotational degrees of freedom (Table 5 and SI Movie). The external and internal entropy terms therefore can be computed separately in our systems. The calculated entropy values are shown in Table 5. A system is well known to lose configuration entropy because the intermolecular attractions inevitably rigidify the 2

molecules on binding.[39,40,64,65] For example, a drug binding to HIV protease can result in >10 kcal/mol entropic penalty from rigidifying conformational and vibrational degrees of freedom.[66] Additional loss of the configuration entropy also comes from translational and rotational entropy of a ligand, >7 kcal/mol, by confining itself in a snug binding site.[57,58] Postanalyzing our MD trajectories showed that all guests and β-CD were not markedly rigidified in the bound state. The guests lost ~1.5–2 kcal/mol external entropy, and β-CD was slightly more flexible, gaining 0.5–1.8 kcal/mol internal entropy with GAFF-CD or being unchanged with q4MD-CD on guest binding (Table 5). Even though different force fields for the host yield considerable differences in β-CD fluctuations, the variation in internal entropy of guests ($-T\Delta S_{\text{Guest Int}}$) is negligible. Also, the interactions between β-CD and guests are not large enough to strongly confine a guest to a handful of well-defined bound guest conformations, thereby allowing a guest to freely tumble and diffuse in the cavity of β-CD. Figure SI 11 illustrates that ligands can pose a wide collection of locations and orientations covering the center and top regions of the binding site, thereby resulting in a small reduction of $-T\Delta S_{\text{Guest Ext}}$.

Changes of Water Entropy on Ligand Binding

Water entropy is one major driving force in ligand binding in these systems, contributing from −2 to −4 kcal/mol to the free energy of binding (Tables 1 and 5). Gaining water entropy dominates in the binding of all guests to β-CD with GAFF-CD and the first 3 weaker binders to β-CD with q4MD-CD. The change in water entropy ($-T\Delta S_{\text{water}}$) is a combined effect from rearranging water molecules, which affects their vibrational and conformational entropy, and from releasing the water molecules residing in the cavity of β-CD or interacting with the guest after the complex is formed (Tables 8 and SI 3–6). We used a grid cell theory approach to calculate the water entropy over the space near the solute, as compared with the entropy estimated for the bulk solvent. We also used an alternative method that computes the molar entropy of water when different solutes are present to approximate $-T\Delta S_{\text{water}}$ (detailed in SI section 6). Both methods agree with each other. The theory and implementation were first validated by comparing our computed molar entropy of bulk water at 298 K, 5.26 kcal/mol (Tables SI 3–5), with the standard molar entropy of water at 298 K, 4.98 kcal/mol. The rigid water TIP3P model performed very well in reproducing standard molar entropy, as reported here and previously, with a two-phase thermodynamic method.[67,68]

Table 5 lists the changes in water entropy on each guest binding to β-CD, and the contribution from each decomposed entropy term is in Tables SI 3–5. Using different force fields to model β-CD did not change the computed $-T\Delta S_{\text{Water}}$, so solute flexibility does not play an important role in water entropy calculations. Aspirin and methyl butyrate have more water entropy gains on binding than do other guests. The 2 guests have more polar functional groups to capture nearby water molecules in their free state, and after forming the complex with β-CD, these water molecules are released, which results in gaining more entropy on binding.

Figure 5 reveals the fluctuation of water molecules presented in the grid space in a pure water box and when β-CD, 2-naphthyl ethanol, or the complex is present using GAFF-CD.

The behavior of water molar entropy in q4MD-CD is similar to GAFF-CD, so only one force field is presented in this figure. The averaged jiggling of water molecules is quantified by computed translational, rotational, and conformational entropy, as shown in columns 2–4 of Figure 5, and the darker grid indicates that water molecules in this cell are less mobile. We used an in-house multilayer visualization program to display the decomposed entropy terms for each grid, and the layer through the center of the solute was selected in the figure. In general, the translational entropy decreases at the surface of the solute because the existence of the solute hinders free diffusion of water molecules. In free β-CD and 2-naphthyl ethanol, the translational entropy of water decreases ~0.2–0.4 kcal/mol around the solutes, as shown by darker cells in the vicinity of each solute in Figures 5B–D.

The rotational entropy increases on the hydrophobic surface and decreases near hydrophilic regions. For example, with free 2-naphthyl ethanol, the rotational entropy increases ~0.2–0.3 kcal/mol near the carbon chains or benzene ring and in the hydrophobic cavity of free and bound β-CD (see lighter cells in Figure 5B and 5C). The nonpolar surface may promote water tumbling, but forming H bonds with a polar group decreases rotational entropy by ~0.2–0.5 kcal/mol near the hydroxyl group of 2-naphthyl ethanol. The conformational entropy is correlated with the density of water molecules (eq 6.6 in SI). The cavity of β-CD is large enough to hold ~5–6 water molecules, on average, and the waters slightly decrease their conformational entropy by 0.2–0.3 kcal/mol because the cavity restrains the rearrangement of water molecules. However, the water is not frozen in the cavity and keeps the fluid-like property, for no significant decrease in translational water entropy. Because the density of water fluctuates during the MD simulations, except for water molecules in the vicinity of solutes, conformational entropy of waters in the bulk solvent or surrounding a solute does not noticeably differ.

Binding Kinetics

Calculations of Association and Dissociation Rate Constants—The fast kinetics of guest binding to β-CD allowed for directly assessing the association (k_{on}) and dissociation (k_{off}) rate constants from the bound and unbound lengths during microsecond-long unguided MD simulations. Table 2 summarizes the calculated k_{on} and k_{off} for systems modeled by GAFF-CD and q4MD-CD. The diffusion-controlled limit for the molecular systems is approximated by $k_{on\_diffuse} = 4\pi DR$, where D is the diffusion coefficient obtained by our MD simulations (4×10^{-9} m^2/s for a guest such as aspirin and 7×10^{-10} m^2/s for β-CD, regardless of force field used) and R is the sum of the radius of β-CD and a guest (~10 Å). The estimated diffusion-controlled association rate constants for all systems are $k_{on\_diffuse} \approx 3–4 \times 10^{10}$ 1/Ms by using the approximated size of each molecule and the diffusion coefficient obtained by MD (Table SI 8). The modeled k_{on} by using GAFF-CD agrees very well with the experimental data, and all guests showed 2 orders of magnitude slower k_{on} than $k_{on\_diffuse}$. Using q4MD-CD slightly overestimated k_{on} for all guest binding, and the value is 1 order of magnitude slower than $k_{on\_diffuse}$ because of the spatial factor. Because β-CD does not require considerable conformational changes or slow transition to acquire all guests, experiments revealed no differences in k_{on} for different guests. However, k_{on} modeled with GAFF-CD shows that larger guests such as aspirin and naphthyl ethanols associate marginally faster to β-CD, with k_{on} values close to 10^9 1/Ms, as compared with

smaller guests such as butanols, with $k_{on} \approx 2–3 \times 10^8$ 1/Ms. The faster association from modeling may result from stronger intermolecular attraction that can more easily retain the guest once 2 molecules collide. In contrast, because k_{on} modeled with q4MD-CD is already fast and close to $k_{on\_diffuse}$, a small difference is observed, with $k_{on} \approx 1–4 \times 10^9$ 1/Ms.

The difference in computed k_{on} with the two force fields and from experimental k_{on} result from the intermolecular attractions and the desolvation process. Guest diffusing on the cyclodextrin surface is unlikely due to weak intermolecular interactions, and the β-CD surface features a restricted target area (window areas). Assuming no intermolecular attraction, successful binding occurs only with the first collision occurring in the window areas of the cavity (~2.5% of the entire surface), which are the areas covering the top and bottom entrance of the cavity. With q4MD-CD, modeled k_{on} is 20 times slower than $k_{on\_diffuse}$, and ~5% of molecular encounters result in successful binding. Therefore, the restricted target area is the main contribution to a slower k_{on}. Using the same concept, less than 1% of the initial association results in a stable complex modeled with GAFF-CD, except for aspirin and 2-naphthyl ethanol. The chief reason that causes further slowdown in k_{on} with GAFF-CD is the desolvation process during association. Although the tilt glucose rings in the free β-CD may partly occlude the cavity, rotating the 2 dihedrals in C–O–C for different glucose ring tilting is nearly barrierless. Replacing water molecules that formed the H-bond network with the free β-CD creates an energy barrier and results in unsuccessful binding, even for a guest already diffused to the cavity. Note, successful binding was considered only when a complex was formed for longer than 1 ns in MD simulations.

In contrast to k_{on}, k_{off} modeled by q4MD-CD agrees very well with experiments; however, with GAFF-CD, all guests left β-CD approximately one order faster than the measured k_{off} values. Because of the faster k_{off}, the equilibrium constants (K_{eq}) are systematically smaller than the experimental values, except for 1-naphthyl ethanol. The dissociation rate constants are directly proportional to how long a guest can stay in the pocket of β-CD, also termed residence time in the drug discovery community. Different force field parameters can largely affect k_{off}. The longer average bound time indicates more negative ΔH (Table 3), in which ΔH computed with q4MD-CD is stronger than that with GAFF-CD. However, longer bound time does not always require stronger intermolecular attractions, and Table 3 shows that the water effects can be the major differentiating factors. Of note, we sampled hundreds of bound/free states during long simulations (Tables SI 10 and 11), but these are still less than the real experiments.

For the weak binders, we observed one direct association/dissociation pathway in which a guest diffused into the window of the cavity and then stayed with β-CD. The association perturbed the conformations of β-CD to get rid of hydrated waters and flip glucopyranose. We term this pathway the direct binding pathway (SI Movies 1, 2, 7, and 8). For the relatively strong binders such as aspirin, for which k_{on} is 3- to 10-fold faster than weak binders modeled by both force fields, we observed one more association/dissociation pathway, termed the sticky binding pathway (SI Movies 3–6 and 9–12). The stronger intermolecular attractions allow the guest to stay on the surface of β-CD for surface diffusion to reach the cavity. This situation largely increases the possibility of binding events because the guests can overcome the limitation of a restricted target area of the surface. Note

that unlike some ligand–protein binding in which the large biomolecular system needs longer than a microsecond time scale for both molecules to arrange to form a complex, binding processes of guest–β-CD are very fast, in the subnanosecond range, without large binding energy barriers. Nevertheless, the intermolecular attractions, possible surface diffusion and desolvation process still play a key role in controlling binding kinetics.

4. DISCUSSION

This study demonstrates that unbiased MD simulations can be used to computeCD–guest binding kinetics and thermodynamics. The kinetic properties and binding enthalpies can be extracted directly from the simulations, but postprocessing of the MD trajectories by using numerical integration and the grid cell method is needed to compute solute and solvent entropy of binding. Computed values with both force fields, GAFF-CD and q4MD-CD, agree well with experimental measures; however, values strikingly differ depending on whether the binding is driven by enthalpy or entropy.

The binding free energy computed from the kinetic data (ΔG_{Comp2}) correlate better with experiments (Figure 2) compared with ΔG_{Comp1} computed from $\Delta H - T\Delta S$. The calculation only needs one long MD run that includes both solutes in one water box. Equation 6 may be rewritten as $\Delta G_{\text{Comp2}} = -RT \ln \left(\frac{1}{\text{average unbound time} \times [\text{solute}]} \cdot C^0 / \frac{1}{\text{average bound time}}\right)$. The numbers of bound and unbound events for computing the average time are nearly identical from the same one MD run; thus, another equation to describe binding free energy may be $\Delta G_{\text{Comp3}} = -RT \ln \left(\frac{\text{total bound time}}{\text{total unbound time} \times [\text{solute}]} \cdot C^0\right)$. From classical statistical mechanics, the probability of observing a bound complex during this long MD run is $P_{\text{bound}} = \frac{\int_{\text{bound}} e^{-E_{\text{bound}}(r)/RT} dr}{\int_{\text{all}} e^{-E(r)/RT} dr}$. As a result, $\Delta G = G_{\text{bound}} - G_{\text{unbound}} = -RT \ln(P_{\text{bound}}/P_{\text{unbound}})$, which is the same as equation ΔG_{Comp3}. The enthalpy change is also available from the average energy of the bound and unbound states in the trajectories of the complexes, $\Delta H_{\text{Bound–unbound}} = \langle H_{\text{bound}} \rangle - \langle H_{\text{unbound}} \rangle$. The computed enthalpy changes are highly similar to the values computed using four separated MD runs (Figure SI 12 and Table 1). This study aims to investigate the kinetic properties in addition to binding affinities; thus, ΔG_{Comp3} was not used to obtain the results. However, for other weak binding systems that k_{on} and k_{off} measurements are not available and for the research that focuses on binding free energies, we suggest that one can run a long MD simulation to obtain ΔG and ΔH. It is worth mentioning that although directly computing entropy changes is not needed if ΔG and ΔH are available, the calculation allows researchers to investigate the water effects in a great detail. The calculations also bring further insights into contributions regarding water entropy and solute configuration entropy to binding. However, because configuration entropy calculations inevitably need multidimension integral, a larger error than ΔG computed from k_{on} and k_{off} is anticipated.

Intuitively, a more negative binding enthalpy ΔH modeled by q4MD-CD is likely a result of the Lennard–Jones parameters, which could result in more optimized $\Delta H_{\text{Host–Guest}}$.[69] Nevertheless, in the decomposed term $\Delta H_{\text{Solute Inter}}$ of $\Delta H_{\text{Host–Guest}}$, the computed

$\Delta H_{\text{Solute Inter (vdW)}}$ and $\Delta H_{\text{Solute Inter (Coul)}}$ show that both force fields model highly similar intersolute attractions, and the main determinant is from water. Both force field parameters allow the sugar ring to flip in the free states, and β-CD can easily adjust to an open cavity conformation when forming a complex with a guest. Therefore, unlike existing study showing that substituents attached to decorated β-CDs block a guest from binding,[70] the ring flipping itself in our study did not hinder guest binding. However, more flipped sugar rings modeled by GAFF-CD allow the formation of more H bonds between waters and β-CD and a more structured H-bond network as compared with conformations modeled by q4MD-CD. Therefore, the cavity more energetically accommodates stable water molecules, which results in large enthalpy penalty on desolvating those water molecules. The Coulombic term $\Delta H_{\text{Host–Water (Coul)}}$ becomes the essential energy term that opposes binding due to breakage of β-CD–water H bonds, and the value is significantly larger with GAFF-CD. We suspected that the bonded parameters with GAFF-CD may highly prefer sugar ring flipping in the free states. However, the MD simulations in vacuum showed that both GAFF-CD and q4MD-CD highly prefer wide-open, crystal structure-like conformations in the free states (Figure SI 1). Because β-CD is reasonably flexible, in particular, with GAFF-CD modeling, adding explicit water molecules easily induces the conformation changes. A “slaving” model in which water drives protein fluctuations was proposed.[71] Recently, a direct measurement of hydration water dynamics in protein systems illustrated that the surface hydration-shell fluctuation drives protein side-chain motions.[72] Here we showed that the water molecules are highly responsible for molecular recognition in both thermodynamics and kinetics.

Without considering other factors, the theoretical k_{on} may be estimated by multiplying the restricted target area by the diffusion-controlled limit $k_{\text{on\_diffuse}}$,[73] $2.5\% \times 4 \times 10^{10}$ 1/Ms = 10^9 1/Ms, which is close to the modeled k_{on} of most guests binding with q4MD-CD. To increase an association rate faster than the theoretical value 10^9 1/Ms, when the initially collision did not bring a guest to the restricted target area, intermolecular attractions kept the guest in close proximity to β-CD until the guest reached the cavity. This situation can be observed during MD simulations, as illustrated in the sticky binding pathways with the relatively tighter binder aspirin. Note no long-range electrostatic attractions for rate enhancement because of the neutral molecules. A guest always needs to compete with water molecules during binding. Therefore, k_{on} can be slower than the theoretical value 10^9 1/Ms if there exist barriers from removing stable water molecules in the hydration shell. The desolvation barrier increases when the free β-CD forms a larger number of H bonds between water molecules modeled by GAFF-CD, which results in more unsuccessful guest binding and slower k_{on}. As a result, although a less wide-open cavity conformation in free β-CD may seem to directly lead to a slower k_{on} in GAFF-CD, the direct cause is from paying a higher cost to disturb its solvation shell. After forming a complex with a guest, β-CD gained a few kcal/mol, showing a more negative $\Delta H_{\text{Host Conf}}$ on binding. A similar finding from investigating binding free energy barriers for a drug binding a protein showed that desolvation of the binding pocket contributes the most to the free energy cost, as opposed to reorganizing the protein binding pocket.[74] However, for molecular systems that encounter large-scale conformational changes and/or induce fit during ligand binding, rearranging conformations may still significantly affect the association rate constants,[75] and the kinetic property can be highly system dependent. With q4MD-CD, because water molecules form a

less stable H-bond network, the role of desolvation in binding kinetics is not as important as with GAFF-CD.

Unlike desolvation effects, which are quite different from the 2 force fields, another dominant but similar driving force for binding from both force fields is the attractive component of the vdW energy, ranging from −6 to −23 kcal/mol. This driving force may be expected because of the nonpolar property of the β-CD cavity and the neutral guests. This term mainly accounts for dispersion forces between β-CD and guests in the force field parameters and is similar for both force fields, with a trend that larger guests have more negative $\Delta H_{\text{Solute Inter (vdW)}}$. In experiments, measuring the separate contributions for binding from dispersive interactions and classical hydrophobic effects in aqueous environment is challenging, and the absolute values from the dispersive interactions are not available experimentally.[76,77] As compared with the vdW attraction, the Coulombic attraction between β-CD and guests is significantly weaker because the guests are not highly charged molecules and few intermolecular H bonds are formed in the complex. The intermolecular attractions are balanced by the enthalpy penalty from disrupting attractions between waters and solutes and gaining water–water enthalpy for those water molecules replaced by a guest, which results in merely a few kcal/mol net enthalpy changes on binding. One may consider hydrophobic effects as the major contributions to β-CD and guest recognition.[78] Of note, although the pocket of β-CD is nonpolar, it is a very tiny cavity and the rims of β-CD consist of several hydroxyl groups. On binding, ~20–25 water molecules were replaced by a larger guest, which agrees with experimental measurement[79] (Table SI 6). However, not all replaced water molecules are “unhappy”. Therefore, although the replaced water molecules also regain water–water attractions in the bulk solvent, the costs to replace the stable water molecules result in the large desolvation penalty. This differs from the binding in a completely hydrophobic cavity, where the enthalpic gain from water–water attraction dominates in the binding process.[80]

The systems did not encounter large solute entropy loss, which contrasts with several existing publications that suggested loss of configuration entropy when a drug binds its target protein.[65,66,81–83] Unlike most drug-like compounds, which fit tightly to their target protein pocket, our guests only loosely fit in the cavity of β-CD. Therefore, the mobility of β-CD is not reduced considerably by a guest. With GAFF-CD, the hydrated water molecules in the cavity of free β-CD showed an ordered H-bond network and slaved the conformational motions of β-CD. On ligand binding, a bound guest did not form a stable H-bond network with β-CD; thus, β-CD showed a slightly increased flexibility. The guests were also able to form various contacts with β-CD. Similar to alternative contacts provided by the hydrophobic binding pocket of protein systems,[84] we did not observe rigidity of β-CD with GAFF-CD.

The enthalpy and entropy balance may follow immediately from eq 5, $\Delta G_{\text{comp1}} = \Delta H - T\Delta S$.[64,85,86] Therefore, it has been suggested that the entropy–enthalpy compensation is from a much smaller range of experimentally measured ΔG for a series of ligands than the range of ΔH. Different from most experimental techniques, we computed the entropy and enthalpy terms separately and still observed the entropy–enthalpy compensation. Our guests were all weak binders and did not have a wide spectrum of ΔG. The computed range of ΔH

is in a similar ballpark as ΔG, and the range of $-T\Delta S$ is relatively smaller than ΔG and ΔH. As a result, the enthalpy change mostly governs if a guest is a stronger or weaker binder. Our calculations reveal the physical basis of larger range of ΔH and more similar $-T\Delta S$. The enthalpy calculations are based on energy functions in the force fields, but the Gibb's entropy formula is based on the distribution of the microstates (eq 1). Unlike protein systems with numerous rotatable bonds and a larger binding site to mostly enclose a ligand, a guest is not completely confined within the cavity of β-CD and the host remains highly flexible. Interestingly, $-T\Delta S_{water}$ is similar in both force fields, and $-T\Delta S_{water}$ is not simply proportional to the size of a guest. Instead, $-T\Delta S_{water}$ relates more to the hydrophilicity of a guest such as 1-propanol, methyl butyrate, and aspirin when forming a complex with β-CD. The free guests reduce more entropy of water in their solvation shell, and these solvation waters gain more entropy on guest binding. For q4MD-CD, because the free β-CD generally has a more open cavity, more waters were released on binding (Table SI 6). However, the ring flipping conformation modeled by GAFF-CD produces a more structured H-bond network for the first hydration shell. As a result, although fewer water molecules were released on binding, those waters gained more entropy than those of β-CD with q4MD-CD, which resulted in a similar computed $-T\Delta S_{water}$ from both force fields. The results suggest that as in enthalpy, entropy calculations feature a fine balance.

Force field parameters are critical for accurate modeling and successful prediction.[87–90] In this study, we used GAFF for β-CD (GAFF-CD) and for all guests and q4md-CD a specialized force field for CDs that combines Amber99SB and GLYCAM04 to match experimental geometries from crystal structures and NMR.[48] It is common practice to seek agreement between the calculated and the experimental binding affinities/binding free energies for validating and improving the parameters of force fields or solvent models. Using computed thermodynamics and kinetics (eqs 5 and 6), both force fields for β-CD showed reasonable agreement with experimental binding affinities, which validated the parameters used. Interestingly, different force fields concluded different driving forces, with GAFF-CD and q4MD-CD showing an entropy- and enthalpy-driven binding, respectively. In addition, GAFF-CD yielded better agreement between computed and experimental association rate constants. Using only binding free energy in the training set for parametrization was suggested to risk an incorrect entropy–enthalpy balance; therefore, binding enthalpy needs to be considered for optimizing parameters.[69] With continuing growth in computer power, for molecular systems with fast association/dissociation rate constants, we suggest considering computed binding kinetics for validating and optimizing force field parameters as well. Our studies also showed the importance of and challenge in correctly modeling multiple conformations in which solvent effects may be remarkable and experimental structures are not available. Although our preliminary studies indicated that using TIP3P and TIP4P water models did not yield different sampled conformations during MD simulations, other molecular systems may be more sensitive to the solvent effects with different water models. In the future, we envision a more careful force field optimization that considers binding free energy, enthalpy–entropy balance, and kinetic properties. We also anticipate further investigation into the role of water in the binding kinetics of various guests to a pocket with different polar and/or nonpolar properties.[91,92]

5. CONCLUSION

In this work, we performed microsecond-time-scale MD simulations with GPU acceleration for 7 chosen β-CD complexes. The computed thermodynamic and kinetic properties agree with experimental values reasonably well. The binding of β-CD complexes is mainly driven by the nonpolar attraction between β-CD and the guest and the entropy gain of desolvated water molecules, regardless of the force field used. With both force fields, the ligands have only a small entropy penalty, and the entropy term also contributes to the binding process. GAFF-CD reproduced more favorable binding entropy and less favorable binding enthalpy due to stronger desolvation penalty than did q4MD-CD. As compared with GAFF-CD, q4MD-CD produced more rigid dynamics of free β-CD. However, the conformational rearrangement did not contribute to the differences in thermodynamics and kinetics modeled by the 2 force fields, and the real determinant was the different H-bond networks between the solvation water molecules and free β-CD. With GAFF-CD, β-CD forms more H bonds with solvation waters in a more distorted conformation; on ligand binding, the ligand needs to pay more enthalpic penalties to remove these stable H-bonded waters, which results in the stronger desolvation enthalpy. In the bound state, free β-CD forms fewer H bonds with its environment and thus becomes more flexible and gains configuration entropy. Although we computed ΔH and $-T\Delta S$ separately, the compensation is observed. In general, hydrogen bonding between water molecules and the solute can significantly influence solute conformations and fluctuations, contribute to desolvation penalty, and slow down the association processes. The water entropy change, which is a fine balance between numbers of released waters and stable waters in the cavity of a receptor, may play an important role in governing ligand–receptor binding. Our study also showed that different force field parameters can yield the same computed ΔG but different entropy and entropy balance.

Supplementary Material

Refer to Web version on PubMed Central for supplementary material.

Acknowledgments

We are thankful for support from the US National Institute of Health (GM-109045), US National Science Foundation (MCB-1350401), and NSF national super computer centers (TG-CHE130009), Dr. Michael Gilson and Dr. Niel Henriksen for insightful discussions on β-cyclodextrin systems, and Dr. Ron Levy for sharing OPLS force field parameters for β-cyclodextrin for our tests. We also thank the anonymous reviewer for valuable comments on the brief version of the manuscript.

References

1. Leavitt S, Freire E. Direct Measurement of Protein Binding Energetics by Isothermal Titration Calorimetry. Curr Opin Struct Biol. 2001; 11(5):560–566. [PubMed: 11785756]
2. Bouchemal K, Mazzaferro S. How to Conduct and Interpret Itc Experiments Accurately for Cyclodextrin-Guest Interactions. Drug Discovery Today. 2012; 17(11–12):623–629. [PubMed: 22326233]
3. Swinney DC. The Role of Binding Kinetics in Therapeutically Useful Drug Action. Curr Opin Drug Discovery Dev. 2009; 12(1):31– 39.
4. Schreiber G, Haran G, Zhou HX. Fundamental Aspects of Protein-Protein Association Kinetics. Chem Rev. 2009; 109(3):839– 860. [PubMed: 19196002]

5. Zhang R, Monsma F. The Importance of Drug-Target Residence Time. Curr Opin Drug Discovery Dev. 2009; 12(4):488–496.
6. Guo D, Mulder-Krieger T, Ijzerman AP, Heitman LH. Functional Efficacy of Adenosine A2a Receptor Agonists Is Positively Correlated to Their Receptor Residence Time. Br J Pharmacol. 2012; 166(6):1846–1859. [PubMed: 22324512]
7. Sykes DA, Dowling MR, Charlton SJ. Exploring the Mechanism of Agonist Efficacy: A Relationship between Efficacy and Agonist Dissociation Rate at the Muscarinic M-3 Receptor. Mol Pharmacol. 2009; 76(3):543–551. [PubMed: 19498041]
8. Tummino PJ, Copeland RA. Residence Time of Receptor- Ligand Complexes and Its Effect on Biological Function (Vol 47, Pg 5481, 2008). Biochemistry. 2008; 47(32):8465–8465.
9. Copeland RA, Pompliano DL, Meek TD. Drug-Target Residence Time and Its Implications for Lead Optimization (Vol 5, Pg 730, 2006). Nat Rev Drug Discovery. 2007; 6(3):249–249.
10. Copeland RA. The Drug-Target Residence Time Model: A 10- Year Retrospective. Nat Rev Drug Discovery. 2016; 15(2):87–95. [PubMed: 26678621]
11. Schneider EV, Boettcher J, Huber R, Maskos K, Neumann L. Structure-Kinetic Relationship Study of Cdk8/Cycc Specific Compounds. Proc Natl Acad Sci U S A. 2013; 110(20):8081–8086. [PubMed: 23630251]
12. Huang, Y-mM, Kang, M., Chang, C-eA. Switches of Hydrogen Bonds During Ligand-Protein Association Processes Determine Binding Kinetics. J Mol Recognit. 2014; 27(9):537–548. [PubMed: 25042708]
13. Cusack KP, Wang Y, Hoemann MZ, Marjanovic J, Heym RG, Vasudevan A. Design Strategies to Address Kinetics of Drug Binding and Residence Time. Bioorg Med Chem Lett. 2015; 25(10): 2019–2027. [PubMed: 25782745]
14. Seow V, Lim J, Cotterell AJ, Yau MK, Xu WJ, Lohman RJ, Kok WM, Stoermer MJ, Sweet MJ, Reid RC, Suen JY, Fairlie DP. Receptor Residence Time Trumps Drug-Likeness and Oral Bioavailability in Determining Efficacy of Complement C5a Antagonists. Sci Rep. 2016; 6doi: 10.1038/srep24575
15. Friedrichs MS, Eastman P, Vaidyanathan V, Houston M, Legrand S, Beberg AL, Ensign DL, Bruns CM, Pande VS. Accelerating Molecular Dynamic Simulation on Graphics Processing Units. J Comput Chem. 2009; 30(6):864–872. [PubMed: 19191337]
16. Shaw DE, Deneroff MM, Dror RO, Kuskin JS, Larson RH, Salmon JK, Young C, Batson B, Bowers KJ, Chao JC, Eastwood MP, Gagliardo J, Grossman JP, Ho CR, Ierardi DJ, Kolossvary I, Klepeis JL, Layman T, McLeavey C, Moraes MA, Mueller R, Priest EC, Shan Y, Spengler J, Theobald M, Towles B, Wang SC. Anton, a Special-Purpose Machine for Molecular Dynamics Simulation. Commun ACM. 2008; 51(7):91–97.
17. Challa R, Ahuja A, Ali J, Khar RK. Cyclodextrins in Drug Delivery: An Updated Review. AAPS PharmSciTech. 2005; 6(2):E329–E357. [PubMed: 16353992]
18. Del Valle EMM. Cyclodextrins and Their Uses: A Review. Process Biochem. 2004; 39(9):1033–1046.
19. Singh M, Sharma R, Banerjee UC. Biotechnological Applications of Cyclodextrins. Biotechnol Adv. 2002; 20(5–6):341– 359. [PubMed: 14550020]
20. Davis ME, Brewster ME. Cyclodextrin-Based Pharmaceutics: Past, Present and Future. Nat Rev Drug Discovery. 2004; 3(12):1023–1035. [PubMed: 15573101]
21. Marchetti L, Levine M. Biomimetic Catalysis. ACS Catal. 2011; 1(9):1090–1118.
22. Breslow R, Dong SD. Biomimetic Reactions Catalyzed by Cyclodextrins and Their Derivatives. Chem Rev. 1998; 98(5):1997– 2011. [PubMed: 11848956]
23. Lai WF. Cyclodextrins in Non-Viral Gene Delivery. Biomaterials. 2014; 35(1):401–411. [PubMed: 24103652]
24. Rekharsky MV, Inoue Y. Complexation Thermodynamics of Cyclodextrins. Chem Rev. 1998; 98(5):1875–1917. [PubMed: 11848952]
25. Izatt RM, Pawlak K, Bradshaw JS, Bruening RL. Thermodynamic and Kinetic Data for Macrocycle Interaction with Cations, Anions, and Neutral Molecules. Chem Rev. 1995; 95(7): 2529–2586.

26. Yim CT, Zhu XX, Brown GR. Kinetics of Inclusion Reactions of Beta-Cyclodextrin with Several Dihydroxycholate Ions Studied by Nmr Spectroscopy. J Phys Chem B. 1999; 103(3):597– 602.
27. Nilsson M, Valente AJM, Olofsson G, Soderman O, Bonini M. Thermodynamic and Kinetic Characterization of Host- Guest Association between Bolaform Surfactants and Alpha- and Beta-Cyclodextrins. J Phys Chem B. 2008; 112(36):11310–11316. [PubMed: 18702539]
28. Fukahori T, Kondo M, Nishikawa S. Dynamic Study of Interaction between Beta-Cyclodextrin and Aspirin by the Ultrasonic Relaxation Method. J Phys Chem B. 2006; 110(9):4487–4491. [PubMed: 16509753]
29. Barros TC, Stefaniak K, Holzwarth JF, Bohne C. Complexation of Naphthylethanols with Beta-Cyclodextrin. J Phys Chem A. 1998; 102(28):5639–5651.
30. Schneider HJ, Hacket F, Rudiger V, Ikeda H. Nmr Studies of Cyclodextrins and Cyclodextrin Complexes. Chem Rev. 1998; 98(5):1755–1785. [PubMed: 11848948]
31. Jana M, Bandyopadhyay S. Hydration Properties of Alpha-, Beta-, and Gamma-Cyclodextrins from Molecular Dynamics Simulations. J Phys Chem B. 2011; 115(19):6347–6357. [PubMed: 21510684]
32. Zhang H, Ge C, van der Spoel D, Feng W, Tan T. Insight into the Structural Deformations of Beta-Cyclodextrin Caused by Alcohol Cosolvents and Guest Molecules. J Phys Chem B. 2012; 116(12): 3880–3889. [PubMed: 22376204]
33. Zoppi A, Quevedo MA, Delrivo A, Longhi MR. Complexation of Sulfonamides with Beta-Cyclodextrin Studied by Experimental and Theoretical Methods. J Pharm Sci. 2010; 99(7):3166–3176. [PubMed: 20166198]
34. Zhang H, Feng W, Li C, Tan T. Investigation of the Inclusions of Puerarin and Daidzin with Beta-Cyclodextrin by Molecular Dynamics Simulation. J Phys Chem B. 2010; 114(14):4876–4883. [PubMed: 20297792]
35. Yeguas V, Altarsha M, Monard G, Lopez R, Ruiz-Lopez MF. Peptide Binding to Beta-Cyclodextrins: Structure, Dynamics, Energetics, and Electronic Effects. J Phys Chem A. 2011; 115(42):11810–11817. [PubMed: 21913730]
36. Henriksen NM, Fenley AT, Gilson MK. Computational Calorimetry: High-Precision Calculation of Host-Guest Binding Thermodynamics. J Chem Theory Comput. 2015; 11(9):4377–4394. [PubMed: 26523125]
37. Zhang H, Yin C, Yan H, van der Spoel D. Evaluation of Generalized Born Models for Large Scale Affinity Prediction of Cyclodextrin Host–Guest Complexes. J Chem Inf Model. 2016; 56(56): 2080–2092. [PubMed: 27626790]
38. Sellner B, Zifferer G, Kornherr A, Krois D, Brinker UH. Molecular Dynamics Simulations of Beta-Cyclodextrin-Aziadamantane Complexes in Water. J Phys Chem B. 2008; 112(3):710–714. [PubMed: 18166034]
39. Wickstrom L, He P, Gallicchio E, Levy RM. Large Scale Affinity Calculations of Cyclodextrin Host-Guest Complexes: Understanding the Role of Reorganization in the Molecular Recognition Process. J Chem Theory Comput. 2013; 9(7):3136–3150. [PubMed: 25147485]
40. Chen W, Chang CE, Gilson MK. Calculation of Cyclodextrin Binding Affinities: Energy, Entropy, and Implications for Drug Design. Biophys J. 2004; 87(5):3035–3049. [PubMed: 15339804]
41. Koehler JEH, Grczelschak-Mick N. The Beta-Cyclodextrin/Benzene Complex and Its Hydrogen Bonds - a Theoretical Study Using Molecular Dynamics, Quantum Mechanics and Cosmo-Rs. Beilstein J Org Chem. 2013; 9:118–134. [PubMed: 23400242]
42. Dinar K, Sahra K, Seridi A, Kadri M. Inclusion Complexes of N-Sulfamoyloxazolidinones with Beta-Cyclodextrin: A Molecular Modeling Approach. Chem Phys Lett. 2014; 595–596:113–120.
43. Liu P, Zhang D, Zhan J. Investigation on the Inclusions of Pcb52 with Cyclodextrins by Performing Dft Calculations and Molecular Dynamics Simulations. J Phys Chem A. 2010; 114(50):13122–13128. [PubMed: 21087060]
44. Lambert A, Yeguas V, Monard G, Ruiz-Lopez MF. What Is the Effective Dielectric Constant in a Beta-Cyclodextrin Cavity? Insights from Molecular Dynamics Simulations and Qm/Mm Calculations. Comput Theor Chem. 2011; 968(1–3):71–76.

45. Pan AC, Xu H, Palpant T, Shaw DE. Quantitative Characterization of the Binding and Unbinding of Millimolar Drug Fragments with Molecular Dynamics Simulations. J Chem Theory Comput. 2017; 13:3372–3377. [PubMed: 28582625]

46. Pedretti A, Villa L, Vistoli G. Vega - an Open Platform to Develop Chemo-Bio-Informatics Applications, Using Plug-in Architecture and Script Programming. J Comput-Aided Mol Des. 2004; 18(3):167–173. [PubMed: 15368917]

47. Wang JM, Wolf RM, Caldwell JW, Kollman PA, Case DA. Development and Testing of a General Amber Force Field. J Comput Chem. 2004; 25(9):1157–1174. [PubMed: 15116359]

48. Cezard C, Trivelli X, Aubry F, Djedaini-Pilard F, Dupradeau F-Y. Molecular Dynamics Studies of Native and Substituted Cyclodextrins in Different Media: 1. Charge Derivation and Force Field Performances. Phys Chem Chem Phys. 2011; 13(33):15103–15121. [PubMed: 21792425]

49. Frisch, MJ., Trucks, GW., Schlegel, HB., Scuseria, GE., Robb, MA., Cheeseman, JR., Scalmani, G., Barone, V., Mennucci, B., Petersson, GA., Nakatsuji, H., Caricato, M., Li, X., Hratchian, HP., Izmaylov, AF., Bloino, J., Zheng, G., Sonnenberg, JL., Hada, M., Ehara, M., Toyota, K., Fukuda, R., Hasegawa, J., Ishida, M., Nakajima, T., Honda, Y., Kitao, O., Nakai, H., Vreven, T., Montgomery, JA., Jr, Peralta, JE., Ogliaro, F., Bearpark, MJ., Heyd, J., Brothers, EN., Kudin, KN., Staroverov, VN., Kobayashi, R., Normand, J., Raghavachari, K., Rendell, AP., Burant, JC., Iyengar, SS., Tomasi, J., Cossi, M., Rega, N., Millam, NJ., Klene, M., Knox, JE., Cross, JB., Bakken, V., Adamo, C., Jaramillo, J., Gomperts, R., Stratmann, RE., Yazyev, O., Austin, AJ., Cammi, R., Pomelli, C., Ochterski, JW., Martin, RL., Morokuma, K., Zakrzewski, VG., Voth, GA., Salvador, P., Dannenberg, JJ., Dapprich, S., Daniels, AD., Farkas, Ö., Foresman, JB., Ortiz, JV., Cioslowski, J., Fox, DJ. Gaussian 09. Gaussian, Inc; Wallingford, CT: 2009.

50. Fenley AT, Henriksen NM, Muddana HS, Gilson MK. Bridging Calorimetry and Simulation through Precise Calculations of Cucurbituril-Guest Binding Enthalpies. J Chem Theory Comput. 2014; 10(9):4069–4078. [PubMed: 25221445]

51. Wang J, Wang W, Kollman PA, Case DA. Automatic Atom Type and Bond Type Perception in Molecular Mechanical Calculations. J Mol Graphics Modell. 2006; 25(2):247–260.

52. Doll JD, Dion DR. Generalized Langevin Equation Approach for Atom-Solid-Surface Scattering - Numerical Techniques for Gaussian Generalized Langevin Dynamics. J Chem Phys. 1976; 65(9): 3762–3766.

53. Adelman SA. Generalized Langevin Theory for Many-Body Problems in Chemical-Dynamics - General Formulation and the Equivalent Harmonic Chain Representation. J Chem Phys. 1979; 71(11):4471–4486.

54. Humphrey W, Dalke A, Schulten K. Vmd: Visual Molecular Dynamics. J Mol Graphics. 1996; 14(1):33–38.

55. Ken, A., Dill, SB. Molecular Driving Forces: Statistical Thermodynamics in Chemistry and Biology. Garland Science; 2003. p. 666

56. Zuckerman, DM. Statistical Physics of Biomolecules: An Introduction. Taylor & Francis; 2010. p. 356

57. Chang CE, Gilson MK. Free Energy, Entropy, and Induced Fit in Host-Guest Recognition: Calculations with the Second- Generation Mining Minima Algorithm. J Am Chem Soc. 2004; 126(40):13156–13164. [PubMed: 15469315]

58. Chang CE, Potter MJ, Gilson MK. Calculation of Molecular Configuration Integrals. J Phys Chem B. 2003; 107(4):1048–1055.

59. Henchman RH. Free Energy of Liquid Water from a Computer Simulation Via Cell Theory. J Chem Phys. 2007; 126(6):064504. [PubMed: 17313226]

60. Irudayam SJ, Henchman RH. Solvation Theory to Provide a Molecular Interpretation of the Hydrophobic Entropy Loss of Noble- Gas Hydration. J Phys: Condens Matter. 2010; 22(28): 284108. [PubMed: 21399280]

61. Gerogiokas G, Calabro G, Henchman RH, Southey MWY, Law RJ, Michel J. Prediction of Small Molecule Hydration Thermodynamics with Grid Cell Theory. J Chem Theory Comput. 2014; 10(1):35–48. [PubMed: 26579889]

62. Fukahori T, Nishikawa S, Yamaguchi K. Kinetics on Isomeric Alcohols Recognition by Alpha- and Beta-Cyclodextrins Using Ultrasonic Relaxation Method. Bull Chem Soc Jpn. 2004; 77(12):2193–2198.

63. Nishikawa S, Fukahori T, Ishikawa K. Ultrasonic Relaxations in Aqueous Solutions of Propionic Acid in the Presence and Absence of Beta-Cyclodextrin. J Phys Chem A. 2002; 106(12):3029–3033.

64. Chodera JD, Mobley DL. Entropy-Enthalpy Compensation: Role and Ramifications in Biomolecular Ligand Recognition and Design. Annu Rev Biophys. 2013; 42:121–142. [PubMed: 23654303]

65. Huang, Y-mM, Chen, W., Potter, MJ., Chang, C-eA. Insights from Free-Energy Calculations: Protein Conformational Equilibrium, Driving Forces, and Ligand-Binding Modes. Biophys J. 2012; 103(2):342–351. [PubMed: 22853912]

66. Chang CEA, Chen W, Gilson MK. Ligand Configurational Entropy and Protein Binding. Proc Natl Acad Sci U S A. 2007; 104(5):1534–1539. [PubMed: 17242351]

67. Lin S-T, Maiti PK, Goddard WA. III Two-Phase Thermodynamic Model for Efficient and Accurate Absolute Entropy of Water from Molecular Dynamics Simulations. J Phys Chem B. 2010; 114(24):8191–8198. [PubMed: 20504009]

68. Pascal TA, Schaerf D, Jung Y, Kuehne TD. On the Absolute Thermodynamics of Water from Computer Simulations: A Comparison of First-Principles Molecular Dynamics, Reactive and Empirical Force Fields. J Chem Phys. 2012; 137(24):244507. [PubMed: 23277945]

69. Yin J, Fenley AT, Henriksen NM, Gilson MK. Toward Improved Force-Field Accuracy through Sensitivity Analysis of Host- Guest Binding Thermodynamics. J Phys Chem B. 2015; 119(32): 10145–10155. [PubMed: 26181208]

70. Tidemand KD, Schonbeck C, Holm R, Westh P, Peters GH. Computational Investigation of Enthalpy-Entropy Compensation in Complexation of Glycoconjugated Bile Salts with Beta-Cyclodextrin and Analogs. J Phys Chem B. 2014; 118(37):10889– 10897. [PubMed: 25158050]

71. Bellissent-Funel MC, Hassanali A, Havenith M, Henchman R, Pohl P, Sterpone F, van der Spoel D, Xu Y, Garcia AE. Water Determines the Structure and Dynamics of Proteins. Chem Rev. 2016; 116(13):7673–7697. [PubMed: 27186992]

72. Qin YZ, Wang LJ, Zhong DP. Dynamics and Mechanism of Ultrafast Water-Protein Interactions. Proc Natl Acad Sci U S A. 2016; 113(30):8424–8429. [PubMed: 27339138]

73. Berg OG, Vonhippel PH. Diffusion-Controlled Macromolecular Interactions. Annu Rev Biophys Biophys Chem. 1985; 14:131–160. [PubMed: 3890878]

74. Mondal J, Friesner RA, Berne BJ. Role of Desolvation in Thermodynamics and Kinetics of Ligand Binding to a Kinase. J Chem Theory Comput. 2014; 10(12):5696–5705. [PubMed: 25516727]

75. Wilson C, Agafonov RV, Hoemberger M, Kutter S, Zorba A, Halpin J, Buosi V, Otten R, Waterman D, Theobald DL, Kern D. Using Ancient Protein Kinases to Unravel a Modern Cancer Drug's Mechanism. Science. 2015; 347(6224):882–886. [PubMed: 25700521]

76. Persch E, Dumele O, Diederich F. Molecular Recognition in Chemical and Biological Systems. Angew Chem, Int Ed. 2015; 54(11):3290–3327.

77. Hobza P. Calculations on Noncovalent Interactions and Databases of Benchmark Interaction Energies. Acc Chem Res. 2012; 45(4):663–672. [PubMed: 22225511]

78. Snyder PW, Lockett MR, Moustakas DT, Whitesides GM. Is It the Shape of the Cavity, or the Shape of the Water in the Cavity? Eur Phys J: Spec Top. 2014; 223(5):853–891.

79. Taulier N, Chalikian TV. Hydrophobic Hydration in Cyclodextrin Complexation. J Phys Chem B. 2006; 110(25):12222– 12224. [PubMed: 16800541]

80. Setny P, Baron R, McCammon JA. How Can Hydrophobic Association Be Enthalpy Driven? J Chem Theory Comput. 2010; 6(9):2866–2871. [PubMed: 20844599]

81. Mobley DL, Dill KA. Binding of Small-Molecule Ligands to Proteins: "What You See" Is Not Always "What You Get". Structure. 2009; 17(4):489–498. [PubMed: 19368882]

82. Silver NW, King BM, Nalam MNL, Cao H, Ali A, Reddy G, Rana TM, Schiffer CA, Tidor B. Efficient Computation of Small-Molecule Configurational Binding Entropy and Free Energy Changes by Ensemble Enumeration. J Chem Theory Comput. 2013; 9(11):5098–5115. [PubMed: 24250277]

83. Forti F, Cavasotto CN, Orozco M, Barril X, Luque FJ. A Multilevel Strategy for the Exploration of the Conformational Flexibility of Small Molecules. J Chem Theory Comput. 2012; 8(5):1808–1819. [PubMed: 26593672]
84. Chang CEA, McLaughlin WA, Baron R, Wang W, McCammon JA. Entropic Contributions and the Influence of the Hydrophobic Environment in Promiscuous Protein-Protein Association. Proc Natl Acad Sci U S A. 2008; 105(21):7456–7461. [PubMed: 18495919]
85. Sharp K. Entropy-Enthalpy Compensation: Fact or Artifact? Protein Sci. 2001; 10(3):661–667. [PubMed: 11344335]
86. Faver JC, Yang W, Merz KM. The Effects of Computational Modeling Errors on the Estimation of Statistical Mechanical Variables. J Chem Theory Comput. 2012; 8(10):3769– 3776. [PubMed: 23413365]
87. Beauchamp KA, Lin YS, Das R, Pande VS. Are Protein Force Fields Getting Better? A Systematic Benchmark on 524 Diverse Nmr Measurements. J Chem Theory Comput. 2012; 8(4):1409– 1414. [PubMed: 22754404]
88. Lindorff-Larsen K, Maragakis P, Piana S, Eastwood MP, Dror RO, Shaw DE. Systematic Validation of Protein Force Fields against Experimental Data. PLoS One. 2012; 7(2):e32131. [PubMed: 22384157]
89. Rauscher S, Gapsys V, Gajda MJ, Zweckstetter M, de Groot BL, Grubmuller H. Structural Ensembles of Intrinsically Disordered Proteins Depend Strongly on Force Field: A Comparison to Experiment. J Chem Theory Comput. 2015; 11(11):5513–5524. [PubMed: 26574339]
90. Wickstrom L, Deng NJ, He P, Mentes A, Nguyen C, Gilson MK, Kurtzman T, Gallicchio E, Levy RM. Parameterization of an Effective Potential for Protein-Ligand Binding from Host-Guest Affinity Data. J Mol Recognit. 2016; 29(1):10–21. [PubMed: 26256816]
91. Setny P, Baron R, Kekenes-Huskey PM, McCammon JA, Dzubiella J. Solvent Fluctuations in Hydrophobic Cavity-Ligand Binding Kinetics. Proc Natl Acad Sci U S A. 2013; 110(4):1197–1202. [PubMed: 23297241]
92. Weiss RG, Setny P, Dzubiella J. Solvent Fluctuations Induce Non-Markovian Kinetics in Hydrophobic Pocket-Ligand Binding. J Phys Chem B. 2016; 120(33):8127–8136. [PubMed: 27009557]
93. Nishikawa S, Ugawa T, Fukahori T. Molecular Recognition Kinetics of Beta-Cyclodextrin for Several Alcohols by Ultrasonic Relaxation Method. J Phys Chem B. 2001; 105(31):7594–7597.

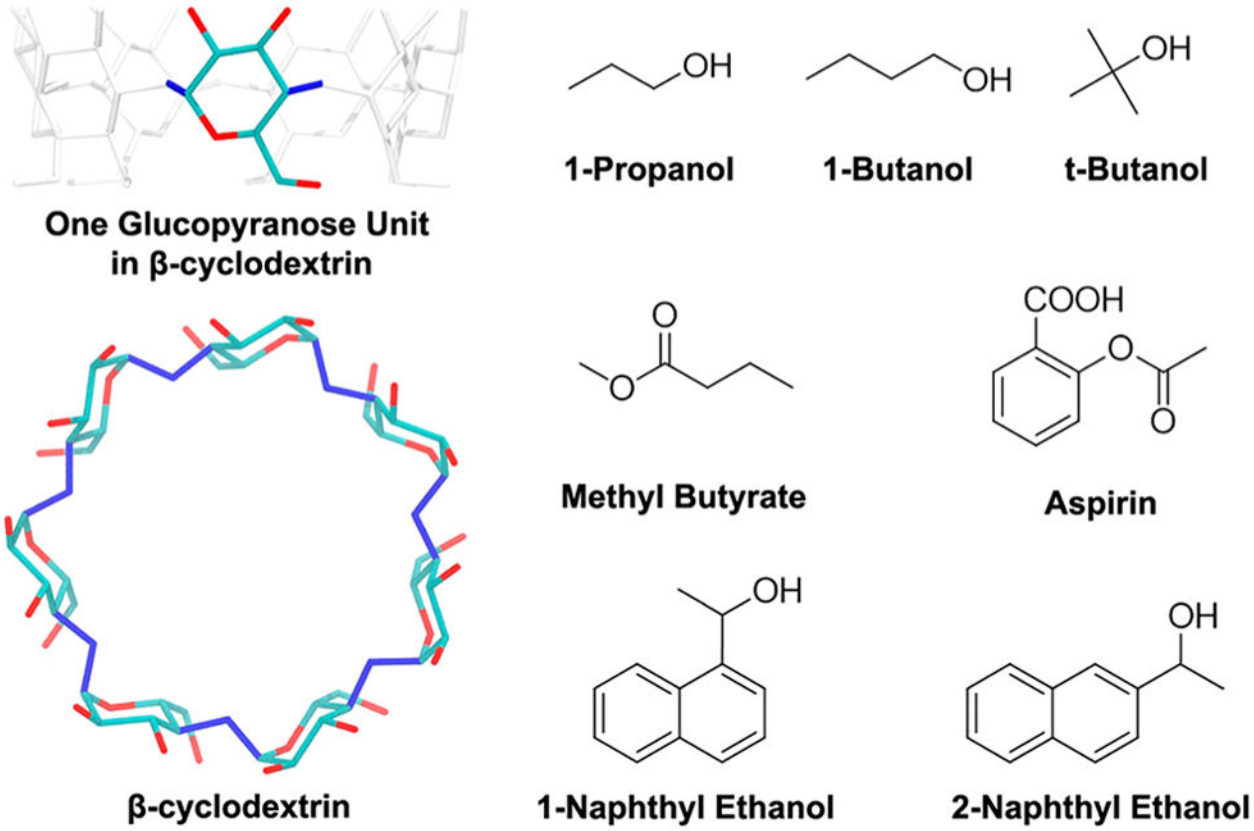

Figure 1.

Structure of β-cyclodextrin (β-CD) and the 7 guest molecules. In the structure of β-CD, hydrogen atoms are not shown. For the β-CD internal (vibrational/conformational) entropy calculation, the 14 dihedral angles used to define the conformations of β-CD are in blue.

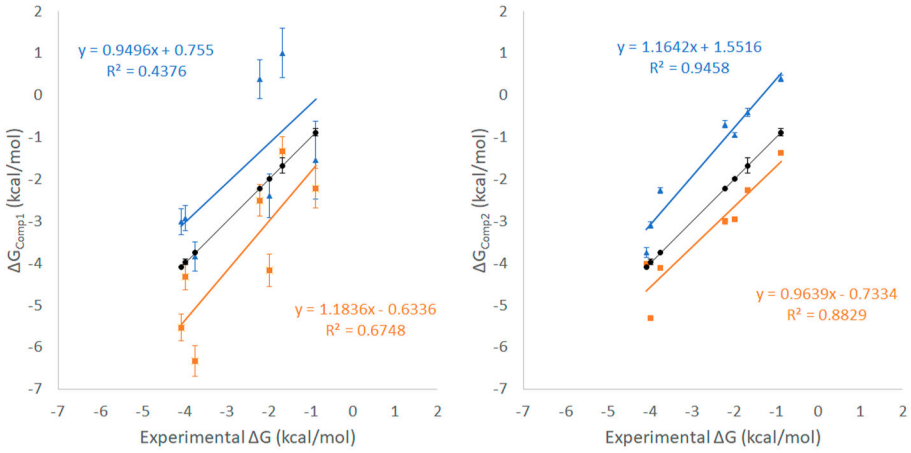

Figure 2.

Correlations between ΔG_{Comp1}, ΔG_{Comp2}, and experimental values. Results from GAFF-CD are shown in blue triangles, and results from q4MD-CD are shown in orange rectangles. Experimental values are shown in black circles. Correlations are labeled correspondingly.

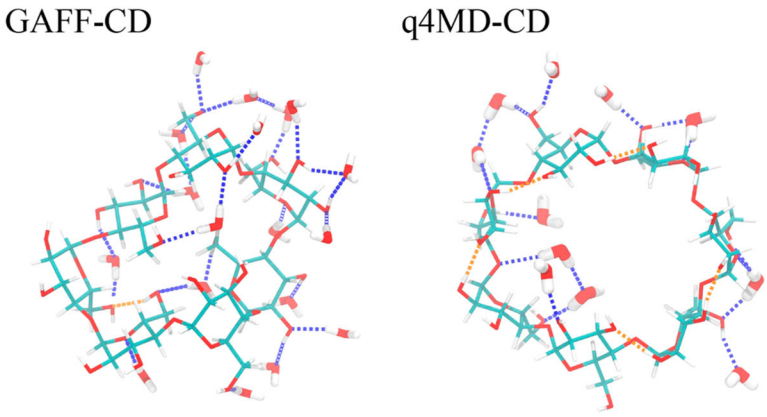

Figure 3.

Hydrogen-bond (H-bond) patterns of representative free β-CD conformations with GAFF-CD and q4MD-CD. With GAFF-CD, there are 18 water molecules forming H bonds with β-CD, 24 H bonds with water (blue dotted lines), and 1 intramolecular H bond (orange dotted lines). With q4MD-CD, there are 11 water molecules forming H bonds with β-CD, 16 H bonds with water, and 5 intramolecular H bonds.

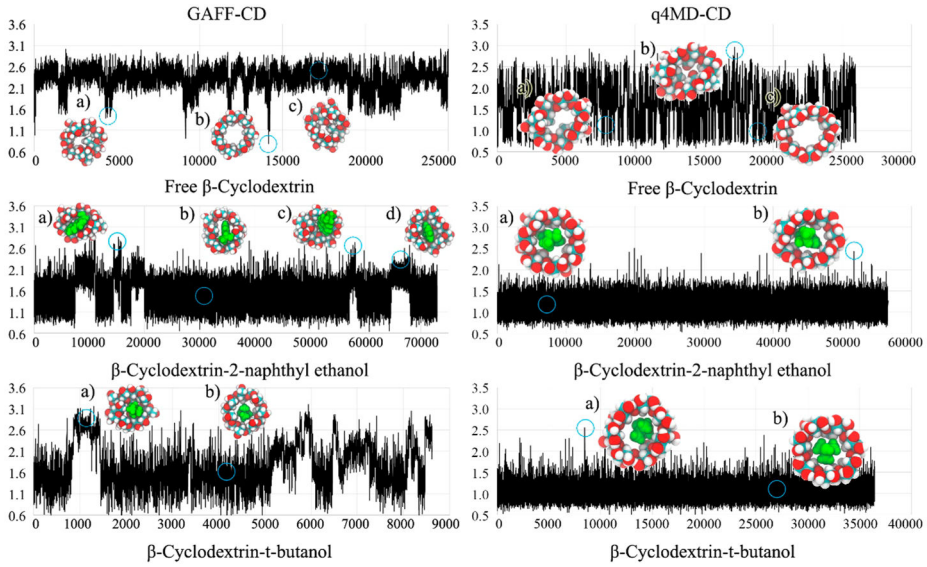

Figure 4.

RMSD plots and representative conformations of β-CD for free β-CD, β-CD-2-naphthyl ethanol complex, and β-CD-*tert*-butanol complex with GAFF-CD and q4MD-CD. RMSD (Å) are computed against the crystal structure by using conformations chosen every 100 ps from all conformations of free β-CD and bound-state conformations of complexes. Representative conformations are shown near the labels (a–d) and circles on the plots. In the representative conformations, ligands are in green.

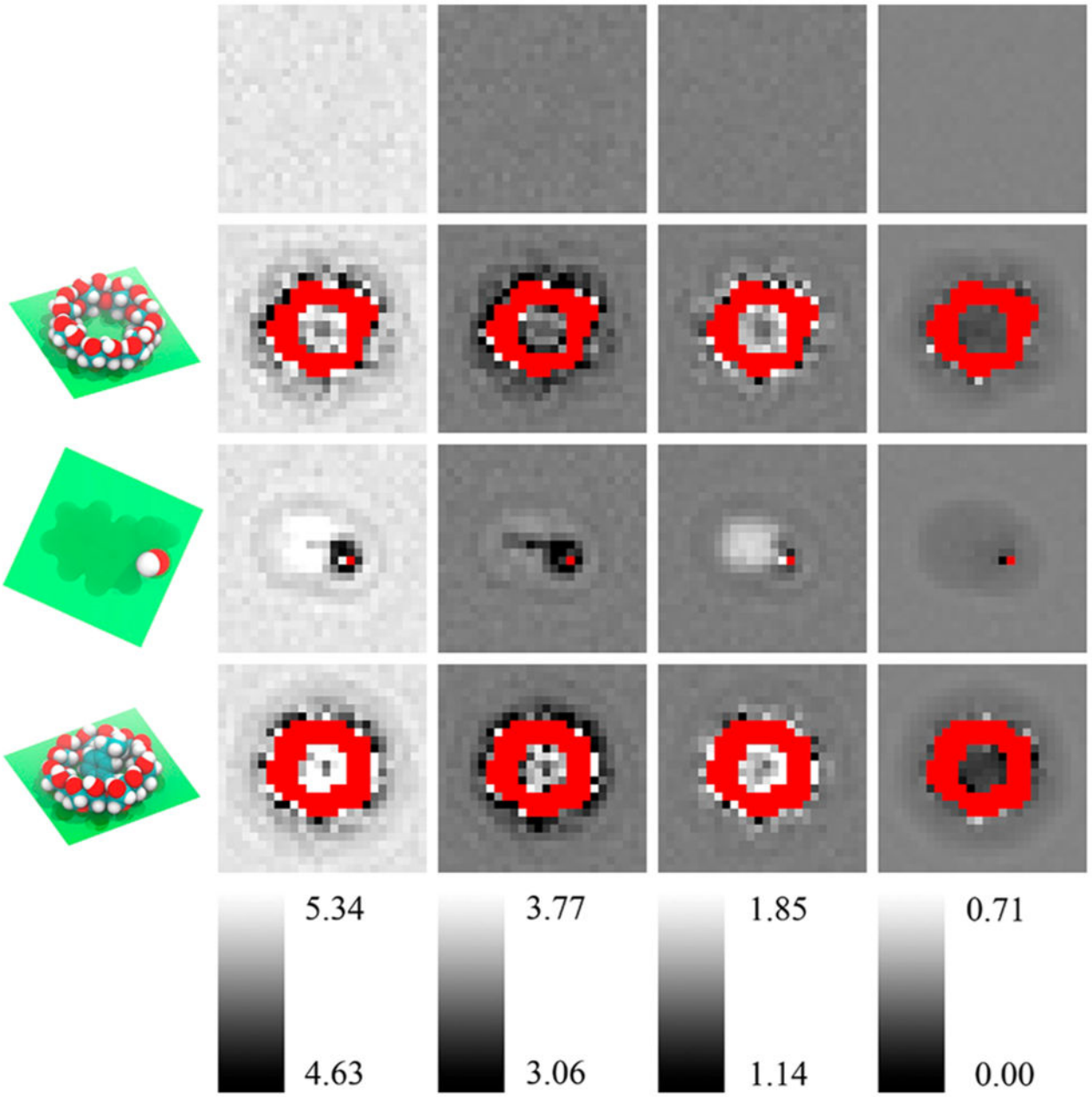

Figure 5.

Water entropy decompositions of pure water and in the vicinities of free β-CD, free 2-naphthyl ethanol, and β-CD-2-naphthyl ethanol complex in GAFF-CD. From top to bottom are pure water (A), free β-CD (B), free 2-naphthyl ethanol (C), and β-CD-2-naphthyl ethanol complex (D). Plane of the spatial grid in the figures is shown in green in the first column. From left to right are total entropy (1, S_{Water}), translational entropy (2, $S_{\text{Water Trans}}$), rotational entropy (3, $S_{\text{Water Rot}}$), and conformational entropy (4, $S_{\text{Water Conf}}$). Each column has a separate color bar (values in kcal/mol). Red areas are regions occupied by the solute molecules, and water entropy cannot be calculated.

Table 1

Binding Free Energies (ΔG), Enthalpies (ΔH), and Entropies ($-T\Delta S$) of β-Cyclodextrin (β-CD) with 7 Guests from Experiments and Calculations by Using GAFF-CD and q4MD-CD Force Fields[a]

calculated (GAFF-CD)			
guest	**ΔG_{Comp1}**	**ΔH**	**$-T\Delta S$**
1-propanol	−1.54 ± 0.93	0.54 ± 0.74	−2.08 ± 0.19
1-butanol	1.01 ± 0.59	2.99 ± 0.52	−1.98 ± 0.06
methyl butyrate	−2.40 ± 0.52	1.88 ± 0.47	−4.29 ± 0.05
tert-butanol	0.38 ± 0.46	2.86 ± 0.40	−2.48 ± 0.06
1-naphthyl ethanol	−3.01 ± 0.31	−1.41 ± 0.28	−1.60 ± 0.03
aspirin	−3.84 ± 0.35	−0.01 ± 0.31	−3.83 ± 0.04
2-naphthyl ethanol	−2.93 ± 0.30	−0.88 ± 0.27	−2.05 ± 0.03
calculated (q4MD-CD)			
guest	ΔG_{Comp1}	ΔH	$-T\Delta S$
1-propanol	−2.21 ± 0.47	−0.66 ± 0.41	−1.55 ± 0.06
1-butanol	−1.33 ± 0.34	−0.85 ± 0.30	−0.48 ± 0.04
methyl butyrate	−4.17 ± 0.38	−2.00 ± 0.33	−2.17 ± 0.05
tert-butanol	−2.50 ± 0.38	−2.87 ± 0.33	0.37 ± 0.05
1-naphthyl ethanol	−5.53 ± 0.32	−5.44 ± 0.29	−0.09 ± 0.04
aspirin	−6.33 ± 0.37	−4.30 ± 0.33	−2.03 ± 0.05
2-naphthyl ethanol	−4.32 ± 0.31	−4.03 ± 0.28	−0.29 ± 0.03
experimental			
guest	ΔG	ΔH	$-T\Delta S$
1-propanol[24]	−0.88 ± 0.09	1.43 ± 0.48	−2.34 ± 0.57
1-butanol[24]	−1.67 ± 0.19	0.69	−2.34
methyl butyrate[63]	−1.99 ± 0.02	/	/
tert-butanol[93]	−2.22 ± 0.01	/	/
1-naphthyl ethanol[29]	−4.08 ± 0.01	/	/
aspirin[28]	−3.74 ± 0.00	/	/
2-naphthyl ethanol[29]	−3.97 ± 0.07	/	/

[a] Unavailable experimental values are marked by /. All values are in kcal/mol.

Table 2

Association and Dissociation Rate Constants of the 7 β-CD Complexes from Experiments and Calculations by Using GAFF-CD and q4MD-CD Force Fields[a]

calculated (GAFF-CD)				
guest	**k_{on} (1/s·M)**	**k_{off} (1/s)**	**K_{eq} (1/M)**	**ΔG_{Comp2} (kcal/mol)**
1-propanol	$2.0 \pm 0.1 \times 10^8$	$3.9 \pm 0.3 \times 10^8$	0.5 ± 0.06	0.40 ± 0.08
1-butanol	$2.2 \pm 0.1 \times 10^8$	$1.1 \pm 0.2 \times 10^8$	2.0 ± 0.3	−0.41 ± 0.10
methyl butyrate	$3.9 \pm 0.1 \times 10^8$	$8.0 \pm 0.6 \times 10^7$	4.9 ± 0.4	−0.94 ± 0.05
tert-butanol	$2.3 \pm 0.1 \times 10^8$	$8.5 \pm 1.2 \times 10^7$	3.2 ± 0.4	−0.69 ± 0.08
1-naphthyl ethanol	$8.6 \pm 1.1 \times 10^8$	$1.5 \pm 1.9 \times 10^6$	558.9 ± 100	−3.75 ± 0.12
aspirin	$1.1 \pm 0.01 \times 10^9$	$2.4 \pm 0.3 \times 10^7$	46 ± 4.3	−2.27 ± 0.06
2-naphthyl ethanol	$9.5 \pm 0.4 \times 10^8$	$5.2 \pm 0.9 \times 10^6$	182 ± 23	−3.08 ± 0.08
calculated (q4MD-CD)				
guest	k_{on} (1/s·M)	k_{off} (1/s)	K_{eq} (1/M)	ΔG_{Comp2} (kcal/mol)
1-propanol	$1.2 \pm 0.02 \times 10^9$	$1.2 \pm 0.02 \times 10^8$	10.1 ± 0.2	−1.37 ± 0.01
1-butanol	$1.5 \pm 0.03 \times 10^9$	$3.3 \pm 0.07 \times 10^7$	45.9 ± 1.2	−2.27 ± 0.02
methyl butyrate	$1.6 \pm 0.1 \times 10^9$	$1.1 \pm 0.1 \times 10^7$	146.8 ± 15	−2.95 ± 0.06
tert-butanol	$1.1 \pm 0.07 \times 10^9$	$7.2 \pm 1.0 \times 10^6$	157.5 ± 18	−3.00 ± 0.07
1-naphthyl ethanol	$1.2 \pm 0.5 \times 10^9$	$1.4 \pm 0.5 \times 10^6$	876.0 ± 42	−4.01 ± 0.03
aspirin	$3.2 \pm 0.3 \times 10^9$	$3.1 \pm 0.9 \times 10^6$	1035.3 ± 83	−4.11 ± 0.05
2-naphthyl ethanol	3.91×10^9	5.0×10^5	7788.3	−5.31
experimental				
guest	k_{on} (1/s·M)	k_{off} (1/s)	K_{eq} (1/M)	ΔG (kcal/mol)
1-propanol[93]	$5.1 \pm 0.7 \times 10^8$	$1.2 \pm 0.07 \times 10^8$	4.2 ± 0.6	−0.88 ± 0.09
1-butanol[93]	$2.8 \pm 0.8 \times 10^8$	$3.8 \pm 0.6 \times 10^7$	7.2 ± 2.0	−1.67 ± 0.19
methyl butyrate[63]	$3.7 \pm 0.3 \times 10^8$	$1.28 \pm 0.03 \times 10^7$	29 ± 1	−1.99 ± 0.02
tert-butanol[93]	$3.6 \pm 0.1 \times 10^8$	$0.85 \pm 0.01 \times 10^7$	42.6 ± 1.0	−2.22 ± 0.01
1-naphthyl ethanol[29]	$4.7 \pm 1.9 \times 10^8$	$4.8 \pm 1.8 \times 10^5$	979 ± 10	−4.08 ± 0.01
aspirin[28]	$7.2 \pm 0.04 \times 10^8$	$1.3 \pm 0.03 \times 10^6$	549 ± 2	−3.74 ± 0.00
2-naphthyl ethanol[29]	$2.9 \pm 1.6 \times 10^8$	$1.8 \pm 0.7 \times 10^5$	820 ± 90	−3.97 ± 0.07

[a]The standard deviations of rate constants of β-CD-2-naphthyl ethanol with q4MD-CD are not available because of lack of adequate binding events.

Table 3

Binding Enthalpy Decompositions of β-CD Complexes by Using GAFF-CD and q4MD-CD Force Fields[a]

calculated (GAFF-CD)									
guest	**ΔH**	**$\Delta H_{\text{Host–Guest}}$**	**$\Delta H_{\text{Host Conf}}$**	**$\Delta H_{\text{Guest Conf}}$**	**$\Delta H_{\text{Solute Inter}}$**	**$\Delta H_{\text{Desolvation}}$**	**$\Delta H_{\text{Host–Water}}$**	**$\Delta H_{\text{Guest–Water}}$**	**$\Delta H_{\text{Water–Water}}$**
1-propanol	0.54	−10.64	−0.87	−0.01	−9.76	11.18	12.20	6.92	−7.93
1-butanol	2.99	−15.28	−2.25	0.00	−13.03	18.27	20.55	8.34	−10.62
methyl butyrate	1.88	−19.31	−2.85	0.02	−16.48	21.19	25.58	10.28	−14.67
tert-butanol	2.86	−15.71	−2.55	−0.04	−13.13	18.57	20.71	8.39	−10.53
1-naphthyl ethanol	−1.41	−30.60	−4.45	0.03	−26.18	29.19	35.45	14.93	−21.19
aspirin	−0.01	−31.53	−3.77	0.23	−27.99	31.52	34.60	19.15	−22.22
2-naphthyl ethanol	−0.88	−28.45	−3.97	0.13	−24.61	27.57	33.21	13.76	−19.40
calculated (q4MD-CD)									
guest	ΔH	$\Delta H_{\text{Host–Guest}}$	$\Delta H_{\text{Host Conf}}$	$\Delta H_{\text{Guest Conf}}$	$\Delta H_{\text{Solute Inter}}$	$\Delta H_{\text{Desolvation}}$	$\Delta H_{\text{Host–Water}}$	$\Delta H_{\text{Guest–Water}}$	$\Delta H_{\text{Water–Water}}$
1-propanol	−0.66	−13.61	−2.05	0.04	−11.60	12.95	13.72	7.74	−8.50
1-butanol	−0.85	−16.66	−2.66	0.09	−14.10	15.82	17.72	9.21	−11.10
methyl butyrate	−2.00	−20.61	−3.53	0.18	−17.26	18.61	22.05	11.10	−14.55
tert-butanol	−2.87	−17.38	−3.50	−0.06	−13.82	14.51	16.31	7.87	−9.67
1-naphthyl ethanol	−5.44	−28.56	−3.42	0.20	−25.34	23.12	29.65	14.51	−21.04
aspirin	−4.30	−29.85	−3.39	0.57	−27.03	25.55	28.91	18.17	−21.53
2-naphthyl ethanol	−4.03	−27.41	−3.38	0.16	−24.20	23.38	28.82	13.95	−19.39

[a]The total binding enthalpy (ΔH) is decomposed into solute–solute interaction change ($\Delta H_{\text{Host–Guest}}$) and desolvation energy ($\Delta H_{\text{Desolvation}}$). $\Delta H_{\text{Host–Guest}}$ includes conformational enthalpy changes of host ($\Delta H_{\text{Host Conf}}$) and guest ($\Delta H_{\text{Guest Conf}}$) and host–guest interaction change ($\Delta H_{\text{Solute Inter}}$). $\Delta H_{\text{Desolvation}}$ decomposes into host–water ($\Delta H_{\text{Host–Water}}$), guest–water ($\Delta H_{\text{Guest–Water}}$), and water–water ($\Delta H_{\text{Water–Water}}$) interaction changes. All values are in kcal/mol.

Table 4

Decompositions of Host–Guest Interaction Change ($\Delta H_{\text{Solute Inter}}$) into van der Waals and Coulombic Energies by Using GAFF-CD and q4MD-CD Force Fields[a]

calculated (GAFF-CD)			
guest	**$\Delta H_{\text{Solute Inter}}$**	**$\Delta H_{\text{Solute Inter (vdW)}}$**	**$\Delta H_{\text{Solute Inter (Coul)}}$**
1-propanol	−9.76	−6.08	−3.68
1-butanol	−13.03	−10.33	−2.7
methyl butyrate	−16.48	−14.33	−2.16
tert-butanol	−13.13	−10.8	−2.32
1-naphthyl ethanol	−26.18	−23.57	−2.61
aspirin	−27.99	−22.76	−5.22
2-naphthyl ethanol	−24.61	−21.72	−2.89
calculated (q4MD-CD)			
guest	$\Delta H_{\text{Solute Inter}}$	$\Delta H_{\text{Solute Inter (vdW)}}$	$\Delta H_{\text{Solute Inter (Coul)}}$
1-propanol	−11.6	−9.67	−1.93
1-butanol	−14.1	−12.09	−2.01
methyl butyrate	−17.26	−15.12	−2.14
tert-butanol	−13.82	−12.39	−1.43
1-naphthyl ethanol	−25.34	−22.76	−2.57
aspirin	−27.03	−22.15	−4.88
2-naphthyl ethanol	−24.2	−21.45	−2.75
Units: kcal/mol			

[a] $\Delta H_{\text{Solute Inter}}$ is decomposed into van der Waals energy ($\Delta H_{\text{Solute Inter (vdW)}}$) and Coulombic energy ($\Delta H_{\text{Solute Inter (Coul)}}$). All values are in kcal/mol.

Table 5

Binding Entropy Decomposition of β-CD Complexes by Using GAFF-CD and q4MD-CD Force Fields[a]

calculated (GAFF-CD)					
guest	$-T\Delta S_{\text{Water}}$	$-T\Delta S_{\text{Host}}$	$-T\Delta S_{\text{Guest Int}}$	$-T\Delta S_{\text{Guest Ext}}$	$-T\Delta S$
1-propanol	−3.32 ± 0.18	−0.52 ± 0.01	0.00 ± 0.00	1.75 ± 0.00	−2.08 ± 0.19
1-butanol	−2.37 ± 0.06	−1.20 ± 0.00	−0.05 ± 0.00	1.64 ± 0.00	−1.98 ± 0.06
methyl butyrate	−4.00 ± 0.04	−1.58 ± 0.00	−0.10 ± 0.00	1.39 ± 0.00	−4.29 ± 0.05
tert-butanol	−2.22 ± 0.05	−1.84 ± 0.00	0.00 ± 0.00	1.57 ± 0.00	−2.48 ± 0.06
1-naphthyl ethanol	−2.28 ± 0.02	−1.24 ± 0.00	0.00 ± 0.00	1.92 ± 0.00	−1.60 ± 0.03
aspirin	−4.08 ± 0.03	−1.53 ± 0.00	0.12 ± 0.00	1.67 ± 0.00	−3.83 ± 0.04
2-naphthyl ethanol	−2.33 ± 0.02	−1.33 ± 0.00	0.00 ± 0.00	1.61 ± 0.01	−2.05 ± 0.03
calculated (q4MD-CD)					
guest	$-T\Delta S_{\text{Water}}$	$-T\Delta S_{\text{Host}}$	$-T\Delta S_{\text{Guest Int}}$	$-T\Delta S_{\text{Guest Ext}}$	$-T\Delta S$
1-propanol	−3.36 ± 0.05	0.21 ± 0.00	0.02 ± 0.00	1.57 ± 0.00	−1.55 ± 0.06
1-butanol	−2.31 ± 0.03	0.25 ± 0.00	−0.17 ± 0.00	1.74 ± 0.00	−0.48 ± 0.04
methyl butyrate	−4.12 ± 0.04	0.22 ± 0.00	−0.11 ± 0.00	1.84 ± 0.00	−2.17 ± 0.05
tert-butanol	−1.84 ± 0.05	0.45 ± 0.00	0.00 ± 0.00	1.76 ± 0.00	0.37 ± 0.05
1-naphthyl ethanol	−2.17 ± 0.03	0.12 ± 0.00	0.00 ± 0.00	1.95 ± 0.01	−0.09 ± 0.04
aspirin	−3.81 ± 0.04	0.11 ± 0.00	−0.16 ± 0.00	1.82 ± 0.00	−2.03 ± 0.05
2-naphthyl ethanol	−2.31 ± 0.03	0.03 ± 0.00	0.00 ± 0.00	1.99 ± 0.01	−0.29 ± 0.03

[a] $-T\Delta S_{\text{Water}}$, $-T\Delta S_{\text{Host}}$, $-T\Delta S_{\text{Guest Int}}$, $-T\Delta S_{\text{Guest Ext}}$, and $-T\Delta S$ are the entropy change of water, internal entropy change of β-cyclodextrin, internal and external entropy change of guests, and the total binding entropy at 298 K. All values are in kcal/mol.

Table 6

Decompositions of β-CD Conformational Enthalpy Change ($\Delta H_{\text{Host Conf}}$) into Bonded, van der Waals, and Coulombic Energies by Using GAFF-CD and q4MD-CD Force Fields[a]

calculated (GAFF-CD)				
guest	**$\Delta H_{\text{Host Conf}}$**	**$\Delta H_{\text{Host Conf (Bonded)}}$**	**$\Delta H_{\text{Host Conf (vdW)}}$**	**$\Delta H_{\text{Host Conf (Coul)}}$**
1-propanol	−0.87	1.37	1.76	−4.00
1-butanol	−2.25	3.97	5.22	−11.44
methyl butyrate	−2.85	4.65	6.01	−13.51
tert-butanol	−2.55	5.05	6.07	−13.67
1-naphthyl ethanol	−4.45	6.23	8.71	−19.39
aspirin	−3.77	5.89	7.95	−17.62
2-naphthyl ethanol	−3.97	5.54	8.15	−17.66
calculated (q4MD-CD)				
guest	$\Delta H_{\text{Host Conf}}$	$\Delta H_{\text{Host Conf (Bonded)}}$	$\Delta H_{\text{Host Conf (vdW)}}$	$\Delta H_{\text{Host Conf (Coul)}}$
1-propanol	−2.05	−0.38	1.79	−3.46
1-butanol	−2.66	−0.38	1.95	−4.23
methyl butyrate	−3.53	−0.47	2.29	−5.34
tert-butanol	−3.50	−0.83	2.18	−4.86
1-naphthyl ethanol	−3.42	0.62	2.57	−6.62
aspirin	−3.39	0.34	2.44	−6.16
2-naphthyl ethanol	−3.38	0.21	2.57	−6.16

[a] $\Delta H_{\text{Host Conf}}$ is decomposed into bonded energy ($\Delta H_{\text{Host Conf (Bonded)}}$), van der Waals energy ($\Delta H_{\text{Host Conf (vdW)}}$), and Coulombic energy ($\Delta H_{\text{Host Conf (Coul)}}$). All values are in kcal/mol.

Table 7

Decompositions of Host–Water ($\Delta H_{\text{Host–Water}}$) and Guest–Water ($\Delta H_{\text{Guest–Water}}$) Interaction Enthalpy Changes into van der Waals and Coulombic Energies by Using GAFF-CD and q4MD-CD Force Fields[a]

calculated (GAFF-CD)						
guest	**$\Delta H_{\text{Host–Water}}$**	**$\Delta H_{\text{Host–Water (vdW)}}$**	**$\Delta H_{\text{Host–Water (Coul)}}$**	**$\Delta H_{\text{Guest–Water}}$**	**$\Delta H_{\text{Guest–Water (vdW)}}$**	**$\Delta H_{\text{Guest–Water (Coul)}}$**
1-propanol	12.20	1.34	10.85	6.92	2.12	4.80
1-butanol	20.55	0.12	20.44	8.34	4.15	4.19
methyl butyrate	25.58	0.64	24.94	10.28	5.79	4.49
tert-butanol	20.71	−1.38	22.09	8.39	4.16	4.23
1-naphthyl ethanol	35.45	0.91	34.54	14.93	9.62	5.32
aspirin	34.60	0.40	34.20	19.15	9.13	10.02
2-naphthyl ethanol	33.21	1.54	31.66	13.76	9.29	4.47
calculated (q4MD-CD)						
guest	$\Delta H_{\text{Host–Water}}$	$\Delta H_{\text{Host–Water (vdW)}}$	$\Delta H_{\text{Host–Water (Coul)}}$	$\Delta H_{\text{Guest–Water}}$	$\Delta H_{\text{Guest–Water (vdW)}}$	$\Delta H_{\text{Guest–Water (Coul)}}$
1-propanol	13.72	4.08	9.63	7.74	3.85	3.89
1-butanol	17.72	5.45	12.27	9.21	4.99	4.22
methyl butyrate	22.05	6.51	15.54	11.10	6.34	4.77
tert-butanol	16.31	4.75	11.56	7.87	5.12	2.75
1-naphthyl ethanol	29.65	8.63	21.02	14.51	9.60	4.91
aspirin	28.91	7.75	21.16	18.17	9.35	8.82
2-naphthyl ethanol	28.82	8.95	19.87	13.95	9.37	4.59

[a] $\Delta H_{\text{Host–Water}}$ and $\Delta H_{\text{Guest–Water}}$ decompose into van der Waals energy ($\Delta H_{\text{Host–Water (vdW)}}$ and $\Delta H_{\text{Guest–Water (vdW)}}$) and Coulombic energy ($\Delta H_{\text{Host–Water (Coul)}}$ and $\Delta H_{\text{Guest–Water (Coul)}}$) terms. All values are in kcal/mol.

Table 8

Decompositions of Water Entropy Change by Using GAFF-CD and q4MD-CD Force Fields[a]

calculated (GAFF-CD)					
guest	$-T\Delta S_{\text{Water Trans}}$	$-T\Delta S_{\text{Water Rot}}$	$-T\Delta S_{\text{Water Vib}}$	$-T\Delta S_{\text{Water Conf}}$	$-T\Delta S_{\text{Water}}$
1-propanol	−2.02	−0.91	−2.92	−0.39	−3.32
1-butanol	−1.18	−0.73	−1.90	−0.47	−2.37
methyl butyrate	−1.92	−1.36	−3.28	−0.72	−4.00
tert-butanol	−1.16	−0.46	−1.63	−0.59	−2.22
1-naphthyl ethanol	−1.12	−0.18	−1.30	−0.98	−2.28
aspirin	−2.36	−0.91	−3.26	−0.82	−4.08
2-naphthyl ethanol	−1.15	−0.24	−1.38	−0.95	−2.33
calculated (q4MD-CD)					
guest	$-T\Delta S_{\text{Water Trans}}$	$-T\Delta S_{\text{Water Rot}}$	$-T\Delta S_{\text{Water Vib}}$	$-T\Delta S_{\text{Water Conf}}$	$-T\Delta S_{\text{Water}}$
1-propanol	−1.93	−0.90	−2.83	−0.53	−3.36
1-butanol	−1.13	−0.47	−1.60	−0.71	−2.31
methyl butyrate	−1.80	−1.46	−3.26	−0.86	−4.12
tert-butanol	−0.77	−0.33	−1.10	−0.74	−1.84
1-naphthyl ethanol	−0.70	−0.37	−1.07	−1.10	−2.17
aspirin	−1.99	−0.86	−2.85	−0.96	−3.81
2-naphthyl ethanol	−0.80	−0.47	−1.26	−1.04	−2.31

[a]The binding water entropy ($-T\Delta S_{\text{Water}}$) decomposes into translational ($-T\Delta S_{\text{Water Trans}}$), rotational ($-T\Delta S_{\text{Water Rot}}$), vibrational ($-T\Delta S_{\text{Water Vib}} = -T\Delta S_{\text{Water Trans}} + -T\Delta S_{\text{Water Rot}}$), and conformational ($-T\Delta S_{\text{Water Conf}}$) terms. All values are in kcal/mol.